ACS Chemical Neuroscience

Article

Rational design and multi-biological profiling of novel donepezil-trolox hybrids against Alzheimer's disease, with cholinergic, antioxidant, neuroprotective and cognition enhancing properties

Pei Cai, Si-Qiang Fang, Xue-Lian Yang, Jia-Jia Wu, Qiao-Hong Liu, Hao Hong, Xiao-Bing Wang, and Lingyi Kong

ACS Chem. Neurosci., **Just Accepted Manuscript** • DOI: 10.1021/acschemneuro.7b00257 • Publication Date (Web): 14 Aug 2017

Rational design and multi-biological profiling of novel donepezil-trolox hybrids against Alzheimer's disease, with cholinergic, antioxidant, neuroprotective and cognition enhancing properties

Pei Cai, [†] Si-Qiang Fang, [†] Xue-Lian Yang, [†] Jia-Jia Wu, [†] Qiao-Hong Liu, [†] Hao Hong, [†] Xiao-Bing Wang, [†]* and Ling-Yi Kong [†]*

[†] *Jiangsu Key Laboratory of Bioactive Natural Product Research and State Key Laboratory of Natural Medicines, China Pharmaceutical University, 24 Tong Jia Xiang, Nanjing 210009, People's Republic of China*

[*]*Corresponding Authors. Tel/Fax: +86-25-83271405; E-mail: cpu_lykong@126.com (Ling-Yi Kong); xbwang@cpu.edu.cn (Xiao-Bing Wang)*

Abstract

A novel series of donepezil-trolox hybrids were designed, synthesized and evaluated as multifunctional ligands against Alzheimer's disease (AD). Biological assays showed that these derivatives possessed moderate to good inhibitory activities against acetylcholinesterase (AChE) and monoamine oxidase B (MAO-B) as well as remarkable antioxidant effects. The optimal compound **6d** exhibited balanced functions with good inhibition against *h*AChE (IC_{50} = 0.54 μM) and *h*MAO-B (IC_{50} = 4.3 μM), significant antioxidant activity (41.33 μM of IC_{50} by DPPH method, 1.72 and 1.79 trolox equivalent by ABTS and ORAC methods), excellent copper chelation and Aβ_{1-42} aggregation inhibition effect. Furthermore, cellular tests indicated that **6d** was very low toxic and capable of combating oxidative toxins (H_2O_2, rotenone and oligomycin-A) induced neurotoxicity. Most importantly, oral administration of **6d** demonstrated notable improvements on cognition and spatial memory against scopolamine-induced acute memory deficit as well as *D*-galactose (*D*-gal) and $AlCl_3$ induced chronic oxidative stress in mice model without acute toxicity and hepatotoxicity. In summary, both *in vitro* and *in vivo* results suggested that **6d** is a valuable candidate for the development of safe and effective anti-Alzheimer's drug.

***Key words*:** Alzheimer's disease, Acetylcholinesterase inhibitors, Antioxidant, β-Amyloid aggregation, Neuroprotection, Cognitive improvement.

1. **Introduction**

Alzheimer's disease (AD) is an age-related neurodegenerative disease featuring in a progressive memory loss, language skills decline and other cognitive impairments.[1] AD has been demonstrated to possess a highly complex network of diverse factors and etiological hallmarks, including the accumulation of abnormal deposits of *β*-amyloid peptide (A*β*), hyperphosphorylated tau protein, neuroinflammation of the central nervous system (CNS), oxidative stress, dyshomeostasis of biometals and low level of acetylcholine (ACh).[2-4] Thus, an appropriate strategy to achieve better therapeutic efficacy for AD is proposed by development of multi-target-directed ligands (MTDLs) that can simultaneously modulate different targets or mechanisms involved in the neurodegenerative AD cascade.[5]

Currently, the dominating treatment agent for AD is acetylcholinesterase inhibitors (AChEIs), which increases the cholinergic neurotransmission in the synaptic cleft by inhibiting degradation of ACh.[6] Also, central acetylcholinesterase (AChE) would play noncholinergic functions in the development of AD. The peripheral anionic site (PAS) of AChE would catalyze A*β* aggregation.[7,8] The aggregation of A*β*, especially A$\beta_{1\text{-}42}$, may lead to the formation of senile plaques in the brain, associated with neurodegeneration.[9] Hence, dual AChEIs which are able to interact with both the catalytic anionic site (CAS) and PAS of AChE are expected not only to alleviate the symptoms, but also to slow down the progression of AD.[10-12]

The hyper-production of reactive oxygen species (ROS) has been observed in AD

and antioxidant enzymes have also been found to be increased in specific AD brain regions.[13] Recently, researches have proved that oxidative damage in cellular structures precedes the appearance of other pathological hallmarks of AD, namely, senile plaques and neurofibrillary tangles.[13-15] In addition, redox-active metal ions like Cu^{2+}, Fe^{2+} and Fe^{3+} is contributed to the production of ROS, which promotes oxidative stress thus leading to AD pathogenesis.[16] Therefore, antioxidant and modulation of such biometals in the brain have been proposed as a promising therapeutic strategy for the treatment of AD.

Donepezil, first choice drug currently used for AD treatment, is among the most popular pharmacophore inspirations in the design of novel drug candidates for its potent, low toxic and well tolerated AChE inhibitory activities.[17] Trolox, a water-soluble analogue of vitamin E, is a powerful antioxidant widely used in biological or biochemical applications to reduce oxidative stress.[18,19] Additionally, it showed neuroprotective effects through scavenging ROS and attenuating the neurotoxicity mediated by Aβ and H_2O_2 on hippocampus neurons.[20-22] These premise of trolox consolidate its neuroprotective capacity and make it an excellent lead compound for the design of multifunctional drugs for treating AD.

In recent years, many interesting MTDLs have been developed, such as, memoquin,[23] ladostigil,[24] and huprine X,[25] among others. Our group has also reported several families of MTDLs that combined neuroprotective, cholinergic, and antioxidant properties, including tacrine–trolox hybrid, melatonin–donepezil hybrids and others.[26,27] Following our previous work and considering both the donepezil and

trolox behaving a very concomitant biological properties for AD treatment, we fused the pharmacophores of donepezil and trolox into one molecule (**Figure 1**). Compounds with zero and two carbon amido linkage were designed to tether these two fragments to meet the requirement of simultaneous binding to PAS and CAS of AChE.[28] The biological activities with regards to the inhibition of ChEs, MAOs and antioxidants activities were evaluated. Noticeably, an optimal compound, **6d**, was assessed neuroprotection in PC12 and BV-2 cells and conducted behavioral performance in mice model of AD.

2. Results and Discussion

2.1. Chemistry

The synthetic method for these derivatives was shown in **Scheme 1**.[29-31] Commercial 4-boc-aminopiperidine (**1**) and 4-(2-boc-aminoethyl)piperidine (**2**) as starting materials were reacted with different substituted benzyl bromides to give the key intermediate **1a-m** and **2a-m**, respectively, then removal of the protecting group with trifluoroaceticacid (TFA) obtained the corresponding 1-benzyl-substituted 4-aminopiperidine **3a-m** and 1-benzyl-substituted 4-aminoethylpiperidine **4a-m** in good yields without further purification. Finally, the target compounds **5a-m** and **6a-m** were prepared by the reaction between trolox and **3a-m** and **4a-m** using *N*-(3-(dimethylamino)propyl)-*N*′-ethylcarbodiimide hydrochloride (EDCI) and 1-hydroxybenzotriazole hydrate (HOBt) as catalyst in dichloromethane (DCM). Structures of all target compounds were characterized by ^{1}H NMR, ^{13}C NMR,

ESI-MS and HRMS.

2.2. Biological Assays.

2.2.1. Inhibitory activities against AChE and BuChE

Cholinesterases (ChEs) in human body comprise of two types, namely, acetylcholinesterase (AChE) and butyrylcholinesterase (BuChE). Normally, AChE hydrolyzes about 80% of acetylcholine while BuChE plays only a secondary role.[32] Therefore, simultaneous inhibition of both AChE and BuChE would be more meaningful for AD treatment.

The inhibitory activities of all target compounds against ChEs were evaluated following the Ellman's method, with donepezil as the reference.[33] Initially, compounds were tested with enzymes from animal source (AChE from electric eel，*ee*AChE, and BuChE from equine serum, *eq*BuChE), considering of the high degree of homology and lower cost compared with human enzymes. As shown in **Table 1**, all target compounds exhibited moderate to good inhibitory towards ChEs. Compound **6a-m** showed more potent inhibitory activity for *ee*AChE than for *eq*BuChE. Conversly, compound **5a-m** exhibited more BuChE selective. Obviously, the length of the alkyl spacer between trolox and donepezil moiety could significantly influence the selective of ChE inhibitory activity. Compound **6d** (*ee*AChE: IC_{50} = 0.31 μM, *eq*BuChE: IC_{50} = 3.91 μM) possessed the most significant bioactivities, revealing 2-F group in the benzene was the best choice for AChE inhibition. Specifically, the AChE inhibition potency of **6a-m** was widely higher than that of **5a-m** having a less-carbon length of alkyl spacer. While the BuChE inhibition was no substantial difference

between **5a-m** and **6a-m**. It may be ascribed to the fact that the functional manner of AChE is different with that of BuChE.[34] Comparing with different substituents (H, CH_3, OCH_3, F, Cl, Br and NO_2), compounds bearing electron-withdrawing group were in favor of the inhibitory activities of AChE. Conversely, the length of the alkyl spacer and substituent effect exhibited no clear trend for BuChE inhibition.

Compounds **6a-m** with potent inhibitory activities for *ee*ChEs were then tested on human ChEs (*h*ChEs) (**Table 1**). It can be observed that compounds **6a-m** were also potent inhibitors of *h*ChEs. Most of these compounds showed decreased inhibitory activity for *h*ChEs compared to *ee*ChEs. Compound **6d** with the inhibitory activity being 0.56 μM was still the most potent inhibitor of *h*AChE.

Table 1. *In vitro* inhibition of AChE and BuChE inhibitory activity of the target compounds.

Compds	n	IC$_{50}$ (μM) [a)]				SI [d)]
		*ee*AChE [b)]	*eq*BuChE [b)]	*h*AChE [c)]	*h*BuChE [c)]	
5a	0	12.53 ± 1.22	5.38 ± 0.02	- [e)]	-	
5b		19.54 ± 0.62	5.49 ± 0.06	-	-	
5c		15.78 ± 0.22	5.94 ± 1.02	-	-	
5d		9.25 ± 0.35	5.88 ± 0.22	-	-	
5e		11.27 ± 0.25	5.42 ± 0.32	-	-	
5f		9.51 ± 0.04	5.32 ± 0.24	-	-	
5g		9.84 ± 0.04	6.01 ± 1.04	-	-	
5h		13.42 ± 0.03	5.93 ± 0.37	-	-	
5i		14.88 ± 1.02	5.15 ± 0.45	-	-	
5j		17.92 ± 1.05	5.83 ± 0.02	-	-	
5k		11.79 ± 0.11	5.66 ± 0.43	-	-	
5l		10.23 ± 0.22	6.73 ± 0.62	-	-	
5m		11.56 ± 0.24	6.34 ± 0.04	-	-	
6a	2	0.82 ± 0.11	3.24 ± 1.01	0.97 ± 0.02	5.62 ± 0.11	5.79
6b		1.63 ± 0.22	3.82 ± 0.90	2.34 ± 0.21	4.91 ± 0.15	2.10
6c		1.44 ± 0.21	3.61 ± 0.81	2.75 ± 0.22	5.80 ± 0.30	2.11
6d		**0.31 ± 0.03**	**3.91 ± 0.11**	**0.56 ± 0.04**	**5.97 ± 0.13**	**10.66**
6e		0.59 ± 0.05	3.87 ± 0.13	1.73 ± 0.06	4.95 ± 0.55	2.86
6f		0.43 ± 0.12	4.09 ± 0.10	1.67 ± 0.09	7.04 ± 1.21	4.43
6g		0.63 ± 0.10	4.54 ± 0.92	1.04 ± 0.01	9.27 ± 1.03	8.91
6h		0.48 ± 0.02	3.69 ± 0.71	2.46 ± 0.02	5.81 ± 0.29	2.26
6i		0.77 ± 0.01	3.71 ± 0.21	2.11 ± 0.09	4.86 ± 1.22	2.30
6j		0.61 ± 0.03	4.58 ± 0.22	1.92 ± 0.05	4.29 ± 0.77	2.55
6k		0.53 ± 0.04	4.52 ± 0.32	1.58 ± 0.08	3.26 ± 0.44	2.06
6l		0.85 ± 0.10	3.94 ± 0.11	1.72 ± 0.32	5.97 ± 0.06	3.47
Donepezil	—	0.07 ± 0.01	2.48 ± 0.11	0.048 ± 0.003	3.17 ± 0.10	66

a) IC$_{50}$: 50% inhibitory concentration (mean ± SD of three experiments);

b) AChE from electric eel and BuChE from equine serum were used;

c) AChE from human erythrocytes and BuChE from human serum were used;

d) SI means selectivity index, *h*BuChE/*h*AChE.

e) Not tested

2. 2. 2. Kinetic study of hAChE inhibition

To assess the *h*AChE inhibition mechanism of donepezil-trolox hybrids, the kinetic test of **6d** was investigated. As presented in **Figure S1 (Supporting Information)**, the Lineweavere-Burk reciprocal plots with increasing slopes and intercepts at higher inhibition concentrations intersected in the fourth-quadrant, indicating a mixed-type inhibitory pattern for compound **6d** to AChE with the inhibition constant Ki of 0.44 μM. Therefore, compound **6d** can simultaneously bind to the CAS and PAS of *h*AChE.[12] The docking results in **Figure S2** (**Supporting Information**) also indicated that compound **6d** could fit into the active-site gorge of the enzyme and simultaneously interact with the PAS and CAS of *h*AChE in agreement with the kinetic study, which demonstrated the rationality of our molecular design.

2.2.3. Inhibitory activities against MAO-A and MAO-B

Monoamine oxidases (MAOs), including MAO-A and MAO-B, catalyze the deamination of amines and are responsible for the regulation and metabolism of major monoamine neurotransmitters.[35] The chemical reaction catalyzed by MAOs resulted in a number of potentially neurotoxic species, such as hydrogen peroxide and ammonia. In particular, hydrogen peroxide can trigger the production of ROS and induce mitochondrial damage and neuronal apoptosis. MAO-B inhibitors have been

considered as rational bases in AD management.[36]

Considering MAOs being highly relevant to oxidative stress, the inhibitory activities on human MAOs (*h*MAOs) of all the target compounds were evaluated. The protocol was carried out with a fluorescence-based method using kynuramine as a nonselective substrate of *h*MAO-A and *h*MAO-B.[37] According to the **Table2**, most of **5a-m** displayed a better inhibition towards *h*MAO-B than *h*MAO-A, while **6a-m** presented unselective action for MAOs. Those suggested the linkage length between two different moieties plays some effects on its selectivity. Compound **5e** was the most active inhibitors (*h*MAO-A: IC_{50} = 9.3 μM, *h*MAO-B: IC_{50} = 1.6 μM). Comparing the two series of compounds, the MAO-B inhibition of **6a-m** was feebly weaker than that of **5a-m**. The results indicated that the linker plays no substantial impacts on the MAO-B inhibitory activity. Additionally, most compounds with the electron-withdrawing groups displayed a increased MAO-B potency.

Table 2. The MAOs inhibition bioactivity and radical scavenging capacity of the target compounds.

Compds	IC_{50} (μM) [a)]			Trolox equivalent [b)]	
	***h*MAO-A**	***h*MAO-B**	**DPPH assay**	**ABTS assay**	**ORAC assay**
5a	15.3 ± 0.2	2.5 ± 0.1	44.38 ± 0.33	1.54 ± 0.22	1.44 ± 0.01
5b	13.1 ± 0.3	3.1 ± 0.2	50.29 ± 1.21	1.51 ± 0.11	1.41 ± 0.02
5c	12.7 ± 0.3	3.3 ± 0.2	50.88 ± 1.52	1.43 ± 0.14	1.47 ± 0.12
5d	8.9 ± 0.1	1.7 ± 0.2	54.30 ± 1.30	1.48 ± 0.12	1.28 ± 0.22
5e	9.3 ± 0.2	1.6 ± 0.3	57.30 ± 2.42	1.59 ± 0.11	1.61 ± 0.12
5f	11.4 ± 0.1	1.8 ± 0.3	58.87 ± 2.43	1.21 ± 0.13	1.29 ± 0.14
5g	11.8 ± 1.2	1.9 ± 0.2	59.64 ± 3.12	1.24 ± 0.11	1.34 ± 0.13
5h	12.5 ± 1.5	2.3 ± 0.5	56.33 ± 2.11	1.12 ± 0.05	1.42 ± 0.08
5i	12.7 ± 2.1	1.7 ± 0.3	52.31 ± 3.45	1.18 ± 0.07	1.28 ± 0.12
5j	13.8 ± 1.5	3.1 ± 0.1	51.90 ± 2.11	1.15 ± 0.05	1.25 ± 0.08
5k	12.6 ± 0.3	2.7 ± 0.9	53.47 ± 3.14	1.21 ± 0.04	1.22 ± 0.08
5l	13.2 ± 0.5	1.9 ± 0.3	51.35 ± 1.21	1.08 ± 0.02	1.28 ± 0.11
5m	11.1 ± 0.4	3.2 ± 0.3	40.77 ± 1.03	1.04 ± 0.03	1.09 ± 0.13
6a	7.8 ± 0.6	7.3 ± 0.2	43.38 ± 1.22	1.76 ± 0.07	1.56 ± 0.02
6b	8.4 ± 0.1	6.9 ± 0.1	47.43 ± 1.22	1.65 ± 0.34	1.45 ± 0.07
6c	8.9 ± 0.1	7.5 ± 0.1	54.90 ± 1.10	1.71 ± 0.08	1.79 ± 0.01
6d	**4.4 ± 0.2**	**4.3 ± 0.2**	**43.33 ± 1.32**	**1.79 ± 0.21**	**1.62 ± 0.03**
6e	5.3 ± 0.5	4.6 ± 0.2	44.99 ± 0.07	1.75 ± 0.02	1.55 ± 0.01
6f	4.8 ± 0.1	4.5 ± 0.3	54.20 ± 1.32	1.68 ± 0.03	1.48 ± 0.02
6g	5.7 ± 0.3	5.8 ± 1.0	49.55 ± 1.89	1.59 ±0.11	1.56 ± 0.02
6h	8.1 ± 0.2	5.3 ± 0.7	44.32 ± 2.43	1.61± 0.04	1.51 ± 0.05
6i	7.2 ± 0.4	6.1 ± 0.4	47.12 ± 3.21	1.54 ± 0.03	1.54 ± 0.06
6j	5.8 ± 0.5	4.8 ±0.3	48.89 ± 3.41	1.49 ± 0.01	1.49 ± 0.10
6k	6.3±0.2	5.7± 0.2	48.24 ± 2.11	1.55 ± 0.05	1.45 ± 0.02
6l	5.4 ± 0.2	4.9 ± 0.1	46.30 ± 2.21	1.60 ± 0.12	1.51 ± 0.05
6m	5.6 ± 0.2	5.1 ± 0.2	47.30 ± 2.20	1.49 ± 0.11	1.57 ± 0.05
Trolox	-	-	45.2 ± 2.30	1	1

a) IC_{50}: 50% inhibitory concentration (means ± SD of three experiments);

b) Data are expressed as (mmol trolox)/(mmol tested compound);

2.2.4. In vitro free radical scavenging activities

As an ample evidence reported, oxidative stress plays an critical role in the development of AD.[13-15] Drugs preventing the formation or clearing of the free radicals in the brain would be beneficial for AD. Three independent approaches, namely, DPPH (diphenyl-1-picrylhydrazyl) radical scavenging method, ABTS (2, 2'-azino-bis(3-ethylbenzthiazoline-6-sulfonicacid)) radical scavenging method and ORAC (oxygen radical absorbance capacity) assay were used to co-elucidate the antioxidant activities of this series of analogs *in vitro*.

2.2.4.1. DPPH radical scavenging assay

DPPH radical can be used in preliminary screening of compounds capable of scavenging reactive oxygen species.[38] For comparison, trolox was used as reference. The results summarized in **Table 2** indicated that all compounds retained the antioxidant activity comparing with trolox. Connecting the trolox with donepezil moiety and variation of substituents did not significantly affect the antioxidant activity, indicating that hybridizing these two scaffolds was rational.

2.2.4.2. ABTS method and ORAC assay

These compounds were also tested for their antioxidant activities by using the ABTS method[39] and ORAC assay.[40] Their antioxidant activities were provided as trolox equivalent (mmol of trolox/mmol of tested compound). As shown in **Table 2**, all the trolox equivalent of the target compounds is larger than 1. It means that most of the compounds demonstrated more superior antioxidant activities compared with

trolox.

Although the antioxidant results from three kinds of free radical scavenging methods performed a little difference, the same trend of free radical scavenging activity was observed according to the results. After above biological evaluation, compound **6d** was chosen as the most promising compound for further study based on its strong and balanced inhibition for both ChEs and antioxidant activity closed to trolox.

*2.2.5. Metal-Chelating properties of compound **6d***

The chelating selectivity and ability of compound **6d** to chelate biometals, such as Cu^{2+}, Zn^{2+}, Fe^{2+} and Fe^{3+}, were studied by UV−vis spectroscopy assay and fluorescence spectrometry.[41] The UV result was presented in **Figure 2A** showed that new optical band was detected at 246 nm after the addition of $CuSO_4$ to the solution of compound **6d**, which demonstrated the production of the corresponding complex via metal chelation. Meanwhile, from the fluorescence spectra in **Figure 2B** (excitation wavelength at 291 nm), the specific fluorescence emission peak of **6d** can be observed at 320 nm with the highest intensity. After Cu^{2+} was added to the HEPES solution of **6d**, the fluorescence intensity of emission spectra was dramatically decreased, and even disappeared in 320nm. The spectra of **6d**-Zn^{2+}, Fe^{2+} and Fe^{3+} were in a moderate decrease of their fluorescence intensity. Overall, the above mentioned different changes indicated that all test metals may possess chelation effect with compound **6d**, especially chelating with Cu^{2+}.

The chelating effect of **6d** for Cu^{2+} in HEPES buffer was further investigated by UV-vis spectrometry. Following the absorption at 246 nm, a series of UV−vis spectra were collected of **6d** titrated with Cu^{2+}, and the isosbestic point demonstrated a 1:1 Cu^{2+}/ligand molar ratio for the unique **6d**-Cu^{2+} complex shown in **Figure 2C** and **Figure 2D** by Job's method.

2.2.6. *Modulation of self- and metal-induced A$\beta_{1\text{-}42}$ aggregation*

we further studied **6d**'s regulation of self- and metal-induced Aβ aggregation by Thioflavin T (ThT) fluorescence assay and transmission electron microscopy (TEM).[42]

The ThT assay results were reported in **Figure 3A**, and the curcumin was used as reference. Compound **6d** inhibited 56.3 ± 4.1% of the self-induced Aβ_{1-42} aggregation and 63.9 ± 3.6% of the Cu^{2+}-induced A$\beta_{1\text{-}42}$ aggregation, which were similar with curcumin (52.9 ± 7.2% and 66.5 ± 3.2%). These results indicated that compound **6d** could effectively inhibit self-induced Aβ aggregation and Cu^{2+}-induced A$\beta_{1\text{-}42}$ aggregation. As indicated in **Figure 3B**, Aβ_{1-42} alone (**Figure 3B-a**) can aggregate into well-defined A$\beta_{1\text{-}42}$ fibrils induced by themselves (**Figure 3B-b**). More complex Aβ fibrils were observed in the presence of Cu^{2+} (**Figure 3B-c**) than with Aβ_{1-42} alone. By contrast, few A$\beta_{1\text{-}42}$ fibrils were observed in the presence of compounds curcumin and **6d** (**Figure 3B-d~g**) under the identical conditions. The consistent results of TEM images and the ThT binding assay suggested that **6d** can inhibit Aβ_{1-42} fibril formation and Cu^{2+}-induced A$\beta_{1\text{-}42}$ aggregation effectively.

*2.2.7. The cytotoxic effect of the compound **6d** on HepG2, PC12 and BV-2 cells*

Considering the critical importance of evaluating the possible hepatotoxicity and the safety index for developing a nervous system drug, we initially screened the cytotoxic effect of **6d** on HepG2, PC12 and BV-2 cells, respectively.[27,43-44]

As presented in **Figure 4A,** compound **6d** displayed negligible hepatotoxicity profile up to 100 μM after 24 h incubation on HepG2 cells and showed no obvious cytotoxicity less than 50 μM on PC12 and BV-2 cells. Collectively, the results suggested **6d** was safe and worthy of further investigations.

*2.2.8. Neuroprotective effect of **6d** against oxidative injuries on PC12 cells*

The over production of ROS and the unbalance in detoxification systems produce severe oxidative stress conditions in neurons affected by AD. Reduction of oxidative stress has been claimed as a viable strategy to slow down the progression of the disease.[13] Therefore, we tested the ability of selected **6d** to protect PC12 cells against oxidative injuries against three different toxic insults (hydrogen peroxide, oligomycin-A and rotenone).

The cytoprotective effect were determined by measuring the cell viability after incubation with a radical initiator (hydrogen peroxide, H_2O_2) and two mitochondrial poisons (oligomycin-A and rotenone), both capable of arresting respiratory chain and energy production.[45] Compound **6d** under investigation was incubated at three concentrations (5, 10 and 20 μM) using the untreated cells as control. As depicted in **Figure 4B**, **6d** exerted a relatively poor neuroprotective activity against cellular

damage induced by oligomycin-A, whereas it showed a moderate to good neuroprotective activity against H_2O_2 and rotenone at the same concentration. **6d** markedly protected PC12 cells against three different toxic insults in a significant dose-dependent manner. These results showed that **6d** was effective against all the oxidative injuries insults on PC12 cells.

*2.2.9. Neuroprotective effects of **6d** against LPS-stimulated inflammation on BV2 microglial cells*

Neuroinflammation plays a crucial role in causing neuronal death and damage, which in turn leads to neurodegenerative diseases such as AD, PD, and multiple sclerosis. The activation of brain microglial cells in the CNS and the subsequent excess production of inflammatory mediators, such as nitric oxide (NO), may result in uncontrolled neuroinflammation in neurodegenerative diseases.[46] Therefore, by inhibiting the production of inflammatory mediators NO in microglial cells, antineuroinflammatory therapy could delay or halt the disease progression prior to irreversible damage and the occurrence of clinical symptoms.

The latest research unclosed that the close relationship was observed between the cholinergic nerves, oxidative stress and inflammation.[47,48] So we determined the antineuroinflammatory properties of **6d** by the Griess assay through detecting the suppression of NO production, using trolox and donepezil as positive control to help illuminate smoothly. Results in **Figure 4C** presented that donepezil and trolox showed lower NO production inhibitory, while **6d** exhibited significantly higher inhibition of

NO production in the LPS-stimulated BV2 cells than the leading compounds trolox and donepezil. The unique structure of **6d** resulted in preferred antineuroinflammatory activities which further stated the rationality of our molecular design.

2.2.10. ***6d*** *reduced LPS-induced intracellular ROS accumulation*

Intracellular ROS act as second messengers in regulating LPS-stimulated production of neurotoxic factors in microglial cells. Correspondingly, specifically inhibiting the production of intracellular ROS is a general way to suppress intracellular proinflammatory signals.[48] As shown in **Figure 4D**, when BV-2 cells were exposed to 1 μg/ml LPS for 18 h, the intracellular ROS increased obviously by using the DCFH-DA probe. While treated with compound **6d,** the level of ROS reduced in a concentration-independent manner. This results suggested that LPS could induce ROS production and **6d** effectively decreased the LPS-induced intracellular ROS accumulation.

Taken together, these all cell-based results highlighted that **6d** was a promising neuroprotective agent and deserved a deeper exploration *in vivo.*

2.2.11. In vitro blood-brain barrier permeation assay

Since brain penetration is essential for successful anti-AD drugs, we evaluated the blood-brain barrier (BBB) penetrating potency of these derivatives. Parallel artificial membrane permeation assay for BBB (PAMPA-BBB) was used according to a previous report by Di *et al.*[49] Assay validation was conducted by comparing

experimental permeability of eight commercial drugs with reported values. A plot of experimental data versus bibliographic values gave a good linear correlation, *Pe* (exp.) = 1.2014*Pe* (bibl.) - 0.3139 (R^2 = 0.9486). From this equation and considering the limit established by Di *et al*. for BBB permeation, we established that compounds with permeability values over 4.5×10^{-6} cm s^{-1} should be able to cross the BBB. From the results presented in **Table S3 (Supporting Information)**, it could be seen that **6d** had the permeability value of 6.7×10^{-6} cm s^{-1}, and exhibited good BBB permeability.

2.2.12. Acute toxicity test and hepatotoxicity studies

Since acute toxicity and hepatotoxicity are two important criterions in new drugs development, the corresponding studies of **6d** was launched. Twenty ICR male mice were randomly allocated into 4 groups, and the test compound **6d** was given in single oral doses of 0, 677, 1333, or 2000 mg/kg, respectively. After administration of the **6d**, mice were monitored continuously for the first 4 h for any abnormal behavior and mortality changes, intermittently for the next 24 h, and occasionally thereafter for 14 days to supervise the onset of any delayed effects. During the experimental period, no acute toxicity symptoms, such as mortality, or unnormal behavior / changes in water or food consumption or body weight were observed (**Figure 5A**). Furthermore, all mice were sacrificed on the 14th day after drug administration, and no damage to the internal organs was macroscopically detected.

Considering that the liver is the main drug metabolic organ, so we further evaluated whether the preferred **6d** had an effect on the liver. After the acute toxicity

study, the heparinized serum of mice of different groups were collected, and the levels of aspartate aminotransferase (AST) and alanine aminotransferase (ALT) were determined. As described in **Figure 5B**, all groups at the experimental doses did not cause significant hepatotoxicity compared to the control, as indicated by no obvious increased activities of ALT and AST. To further confirm its non-hepatotoxicty, morphological study of the highest dosage on liver tissue stained with hematoxylin and eosin (HE) was performed. Results showed that no significant area of necrosis and distinct fatty degeneration of the hepatocytes or other substantial lesions were observed (**Figure 5C**), which means no signally morphological changes after the treatment with 14d even in the highest concentration. These results were consistent with the previous HepG2 cell model evaluation. All the results co-illuminate the **6d** had no acute hepatotoxicity and possessed similar safety index to donepezil and trolox for the treatment of AD. Overall, compound **6d** had no acute toxic and well tolerated at doses up to 2000 mg/kg.

2.2.13. Cognitive and memory improvement test of scopolamine-induced cognition impairment

Cognition-improving potency is of utmost importance for anti-AD agents. Compound **6d's** ability to ameliorate scopolamine-induced cognition impairment in ICR mice was investigated in a behavioral study using the step-through passive avoidance test and the Morris water maze test.[50-52] Donepezil and **6d** were orally administered to the ICR mice 30 min before intraperitoneal (i.p.) administration of

scopolamine (3 mg/kg) or saline solution for 10 consecutive days to adapt the apparatus.

2.2.13.1 Passive avoidance task

Firstly, the step-through passive avoidance test was used to assess **6d** cognition-improving potency. As shown in **Figure 6A**, the step-through latency of mice treated with scopolamine alone (model group) was significantly shorter than that of vehicle-treated mice (control group), which means the scopolamine-induced cognition impairment has been established. The treatment with **6d** (5mg/kg, 10mg/kg, 20mg/kg) significantly increased the latency time in a dose-dependent manner. In particular, the effect of **6d** (20 mg/kg) was comparable with that of donepezil (5 mg/kg). These results indicated that **6d** can reverse cognitive deficit against scopolamine-induced cognition impairment.

2.2.13.2 Morris water maze test

After the preliminary evaluation of compound **6d** cognition-improving effect by passive avoidance task, we further confirmed by Morris water maze test which is the most common and recognized widely in assessing the learning and memory ability. During the training trials, the mean escape latency and searching distance for the mice in each group declined progressively; however, the model mice normally spent more time and required farther distance to find the hidden platform. **Figure 6B-a** showed the mean values of the escape latencies to the hidden platform at day 1 and day 5. Control-operated mice exhibited a reduction of mean escape latency from 47.3 to 19.4 s over the course of five training days. Compared with the control group, the high

dosage **6d**-treated group (20mg/kg) had similar escape latency to donepezil treated group, displaying a reduction of mean escape latency from 54.9 to 24.3 s, which the donepezil group showed a reduction from 47.6 to 23.9 s. Meanwhile, the average swimming speed (**Figure 6B-b**) for each group of mice was virtually equivalent, which further demonstrated that the long-term uptake of **6d** did not impact the animals' normal physiology activity. Furthermore, in the probe trial on day 6, the administration of **6d** improved the overall target quadrant preference (28.88%) compared with the model group (20.62%) (**Figure 6B-c**). Also, the **Figure 6B-d** indicated that the control group had significantly higher numbers of virtual platform (the original platform location) crossings (3.6 ± 0.6) compared to the model group mice (1.5 ± 0.4), which strongly suggested that scopolamine led to a spatial memory deficiency in the mice. The numbers of virtual platform crossings for the mice that were administered donepezil (3.0 ± 0.5), **6d** (3.5 ± 0.8) were remarkably improved compared to the model group. The representative tracks of the mice in Morris water maze during the spatial probe trial period (**Figure 6B-e)** formed a more clear and definite spatial preference in the correct quadrant of the platform. These results further revealed that administration of **6d** led to a substantial improvement of the conventional reference spatial memory and cognitive abilities.

2.2.14. Cognitive and memory improvement test of D-gal and $AlCl_3$-induced chronic cognition impairment

Reports has demonstrated that the combination of *D*-galactose (*D*-gal) and $AlCl_3$

eventually damages learning and memory as well as increased production of ROS.[53, 54] Therefore, mice continuously treated with *D*-gal and $AlCl_3$ might be a better model for studying the mechanisms of AD and for drug screening.

To investigate the effects of **6d** on *D*-gal and $AlCl_3$ induced cognitive impairment, trolox and **6d** were orally administered to the ICR mice for 40 consecutive days, and from the 15th day, *D*-gal (150mg/kg/d) and $AlCl_3$ (10mg/kg/d) were intraperitoneal injectioned after 6 h giving the compounds. A spatial memory test was subsequently performed as previously described by passive avoidance task. The step-through latency of mice treated with *D*-gal and $AlCl_3$ alone (model group) was significantly shorter than that of control-treated mice. As reported in **Figure 7A**, the treatment with **6d** (20mg/kg) significantly increased the latency time compared with model group. The effect of **6d** was slightly superior to trolox (20mg/kg). In particular, it did not cause any adverse or abnormal events (such as emesis-like or diarrhea behavior) or affect the survival. The results were also proved by intuitional histopathological studies for hippocampal neurons as showed in **Figure 7C**. The control group demonstrated significant neuronal normalities, while the model's presented with nuclear pyknosis, neuronal shrinkage and an irregular shape, which indicated a necrotic morphology. In the trolox and **6d** group, fewer significant neuronal abnormalities were detected in the hippocampus. These results indicated that **6d** can reverse and protect cognitive deficit of *D*-gal and $AlCl_3$-induced chronic cognition impairment to some extent.

2.2.15 Estimation of biochemical parameters

To further verify **6d**'s effects on this chronic oxidative stress model, we determined the biochemical parameters related to oxidative damages.[55, 56] After the behavior assessments, the mice were sacrificed, and the brain were collected rapidly, rinsed with cold phosphate-buffered saline (PBS). The biochemical parameters in different groups were shown in **Figure 7B**. The levels of malondialdehyde (MDA), the oxidative stress markers, exhibited a significant increase in the model group compared with the control group. **6d** treatment significantly decreased the enhanced levels of MDA in model mice (**Figure 7B-a**). The model group had a notable reduction in the quantity of superoxide dismutase (SOD) (**Figure 7B-b**), the activities of glutathione peroxidase (GSH-PX) (**Figure 7B-c**) were significantly inhibited in model groups compared with the normal groups, which were greatly reversed by compound **6d**.

The above impressive profile maybe attribute to the facts that **6d** increased brain cholinergic activity by inhibition of AChE and protected the cholinergic nerve owing to its significant neuroprotective effects.

3. Conclusion

This study involved the design, synthesis and biological evaluation of a series of multifunctional agents against AD by fusing the pharmacophore of donepezil and trolox. Among all the compounds, compound **6d** behaved balanced functions with excellent *h*AChE inhibition and MAO-B inhibition, efficient antioxidant capacity by

DPPH, ABTS and ORAC assays, significant copper chelating properties and effective inhibitory activity against self- and Cu^{2+}-induced Aβ_{1-42} aggregation. Furthermore, cellular tests indicated that **6d** was very low toxic on three cells models (HepG2, PC12 and BV-2) and capable of combating oxidative toxins (H_2O_2, rotenone and oligomycin-A) induced neurotoxicity on PC12 cells. Besides, **6d** presented a significant effect on protecting neuronal cells against LPS-stimulated inflammation on BV-2 cells. Most importantly, oral administration of **6d** demonstrated notable improvements on cognition and spatial memory against scopolamine-induced acute memory deficit as well as *D*-galactose (*D*-gal) and $AlCl_3$ induced chronic oxidative stress models in mice without acute toxicity and hepatotoxicity. A hypothetical scheme for the pharmacologic mechanisms of **6d** in the treatment of Alzheimer's disease mice model was summarized in **Figure S5 (Supporting Information**) in which **6d** played good profile through its good cholinergic and noncholinergic pathways. Altogether, both the results *in vitro* and *in vivo* suggested that **6d** was a valuable candidate for the development of safe and effective anti-Alzheimer's drug.

4. Methods

4.1 Chemistry

4.1.1 General methods

All common reagents and solvents were obtained from commercial suppliers and used without further purification. Reaction progress was monitored using analytical thin layer chromatography (TLC) on precoated silica gel GF254 plates (Qingdao

Haiyang Chemical Plant, Qingdao, China) and detected under UV light (254 nm). Column chromatography was performed on silica gel (90–150 mm; Qingdao Marine Chemical Inc.). ^{1}H NMR and ^{13}C NMR spectra were measured with a Bruker ACF-500 spectrometer at 25 °C and referenced to TMS. Chemical shifs are reported in ppm (δ) using the residual solvent line as the internal standard. Mass spectra were obtained with an Agilent 1100 Series LC/MSD Trap mass spectrometer (ESI-MS) and a Mariner ESI-TOF spectrometer (HRESI-MS), respectively.

*4.1.2 General procedures for the preparation of 5**a-m*** and ***6a-m***

The commercially available starting material **1** and **2** (1.0 mmol) was respectively suspended in ethyl alcohol (10 mL) containing triethylamine (TEA) (2.0 mmol). The reaction was treated with appropriately substituted benzyl bromides (1.2 mmol) and heated under reflux for 8 h to give the key intermediate **1a-m** and **2a-m**, then the product was treated with trifluoroaceticacid (TFA) (4eq) to give 1-benzyl-substituted 4-aminopiperidine **3a-m** and 1-benzyl-substituted 4-aminoethylpiperidine **4a-m** in good yields without further purification. Finally, trolox (1eq) were reacted with **3a-m** and **4a-m** in dichloromethane (DCM) with *N*-(3-(dimethylamino)propyl)-*N*′-ethylcarbodiimide hydrochloride (EDCI) (1eq) and 1-hydroxybenzotriazole hydrate (HOBt) (1eq) catalytic system at room temperature for 12h. The reaction mixture was washed with saturated aqueous solution of sodium bicarbonate and extracted with DCM. The combined organic layers were dried over anhydrous Na_2SO_4 and evaporated under vacuum. Purification of the crude product was achieved by column chromatography. Structures of all targeted compounds were

characterized by ^{1}H NMR, ^{13}C NMR, ESI-MS and HRMS.

*6-hydroxy-N-(1-(4-methoxybenzyl)piperidin-4-yl)-2,5,7,8-tetramethylchromane-2-carboxamide (**5a**)*

Yield 37%, white oil. ^{1}H NMR (500 MHz, DMSO-d_6) δ 7.56 (s, 1H), 7.20 – 7.10 (m, 4H), 6.83 (d, J = 7.5 Hz, 1H), 3.72 (s, 3H), 3.65 – 3.62 (m, 1H), 3.28 (dd, J = 11.8, 5.1 Hz, 2H), 2.58 – 2.53 (m, 1H), 2.44 (d, J = 7.0 Hz, 2H), 2.22 (dt, J = 11.8, 8.1 Hz, 2H), 2.13 (s, 3H), 2.12 (s, 3H), 2.01 (s, 3H), 1.78 – 1.65 (m, 2H), 1.47 – 1.42(m, 2H), 1.41 (s, 3H), 1.23-1.20 (m, 3H). ^{13}C NMR (151 MHz, DMSO-d_6) δ 173.01, 146.49, 144.28, 130.46, 129.90, 127.41, 125.80, 123.16, 121.29, 120.87, 117.72, 77.74, 60.61, 55.60, 31.22, 30.00, 24.62, 20.63, 19.22, 13.38, 12.47, 12.27. ESI-MS *m/z*: 453.3 $[M+H]^+$; HRMS (ESI) *m/z* 453.2750 $[M+H]^+$ (calcd for 453. 2753, $C_{27}H_{37}N_2O_4$).

*6-hydroxy-2,5,7,8-tetramethyl-N-(1-(2-methylbenzyl)piperidin-4-yl)chromane-2-carboxamide (**5b**)*

Yield 30%, white oil. ^{1}H NMR (500 MHz, DMSO-d_6) δ 7.56 (s, 1H), 7.30 – 7.12 (m, 4H), 6.80 (d, J = 7.5 Hz, 1H), 3.58 – 3.55 (m, 1H), 3.25 (dd, J = 12.4, 5.1 Hz, 2H), 2.58 – 2.54 (m, 1H), 2.44 (d, J = 7.0 Hz, 2H), 2.30 (s, 3H), 2.22 (dt, J = 11.8, 8.1 Hz, 2H), 2.13 (s, 3H), 2.12 (s, 3H), 2.01 (s, 3H), 1.78 – 1.75 (m, 2H), 1.49 – 1.44 (m, 2H), 1.41 (s, 3H), 1.25 – 1.21 (m, 3H). ^{13}C NMR (151 MHz, DMSO-d_6) δ 173.01, 146.49, 144.28, 130.46, 129.90, 127.41, 125.80, 123.16, 121.29, 120.87, 117.72, 77.74, 60.61, 31.22, 30.00, 24.62, 20.63, 19.22, 13.38, 12.47, 12.27. ESI-MS *m/z*: 437.3 $[M+H]^+$; HRMS (ESI) *m/z* 437.2797 $[M+H]^+$ (calcd for 437.2799, $C_{27}H_{37}N_2O_3$).

6-hydroxy-2,5,7,8-tetramethyl-N-(1-(4-methylbenzyl)piperidin-4-yl)chromane-2-c

*arboxamide (**5c**)*

Yield 43%, pale yellow oil. ^{1}H NMR (500 MHz, DMSO-d_6) δ 7.54 (s, 1H), 7.25 – 7.11 (m, 4H), 6.81 (d, J = 7.5 Hz, 1H), 3.65 – 3.62 (m, 1H), 3.26 (dd, J = 12.1, 4.1 Hz, 2H), 2.58 – 2.56 (m, 1H), 2.45 (d, J = 7.0 Hz, 2H), 2.30 (s, 3H), 2.25 – 2.21(m, 2H), 2.13 (s, 3H), 2.12 (s, 3H), 2.01 (s, 3H), 1.76 – 1.75 (m, 2H), 1.45 – 1.40 (m, 2H), 1.41 (s, 3H), 1.33 – 1.23 (m, 3H). ^{13}C NMR (151 MHz, DMSO-d_6) δ 173.01, 146.49, 144.28, 130.46, 129.90, 127.41, 125.80, 123.16, 121.29, 120.87, 117.72, 77.74, 60.61, 31.22, 30.00, 24.62, 20.63, 19.22,13.38, 12.47, 12.27. ESI-MS *m/z*: 437.3 $[M+H]^+$; HRMS (ESI) *m/z* 437.2796 $[M+H]^+$ (calcd for 437.2799, $C_{27}H_{37}N_2O_3$).

*N-(1-(2-fluorobenzyl)piperidin-4-yl)-6-hydroxy-2,5,7,8-tetramethylchromane-2-c arboxamide (**5d**)*

Yield 47%, pale yellow oil.^{1}H NMR (500 MHz, DMSO-d_6) δ 7.58 (s, 1H), 7.34 – 7.29 (m, 3H), 7.23 (d, J = 7.3 Hz, 1H), 6.83 (d, J = 7.0 Hz, 1H), 3.61 – 3.55 (m, 1H), 3.31 (d, J = 14.1 Hz, 1H), 3.22 – 3.20(m, 1H), 2.57 (d, J = 5.9 Hz, 1H), 2.46 – 2.43 (m, 2H), 2.21 (dt, J = 14.1, 7.4 Hz, 2H), 2.13 (s, 3H), 2.12 (s, 3H), 2.01 (s, 3H), 1.78 – 1.76 (m, 2H), 1.49 (dd, J = 10.6, 7.3 Hz, 2H), 1.41 (s, 3H), 1.27 – 1.25 (m, 3H). ^{13}C NMR (151 MHz, DMSO-d_6) δ 161.87 – 161.74, 146.45, 144.22, 142.30, 130.51, 125.19, 123.28, 121.40, 120.90, 117.73, 115.38, 114.00 – 113.86, 77.74, 61.81, 31.29, 29.95, 24.52, 20.50, 13.32, 12.46, 12.26. ESI-MS *m/z*: 441.3 $[M+H]^+$; HRMS (ESI) *m/z* 441.2550 $[M+H]^+$ (calcd for 441.2548, $C_{26}H_{34}FN_2O_3$).

*N-(1-(3-fluorobenzyl)piperidin-4-yl)-6-hydroxy-2,5,7,8-tetramethylchromane-2-c arboxamide (**5e**)*

Yield 47%, white oil. ^{1}H NMR (500 MHz, DMSO-d_6) δ 7.58 (s, 1H), 7.34 – 7.30 (m, 3H), 7.23 (d, J = 7.3 Hz, 1H), 6.83 (d, J = 7.0 Hz, 1H), 3.61 – 3.58 (m, 1H), 3.32 (d, J = 12.1 Hz, 1H), 3.24 – 3.21 (m, 1H), 2.59 (d, J = 7.4 Hz, 1H), 2.45 – 2.43 (m, 2H), 2.20 (dt, J = 11.9, 7.4 Hz, 2H), 2.13 (s, 3H), 2.12 (s, 3H), 2.01 (s, 3H), 1.72 – 1.69 (m, 2H), 1.48 – 1.47 (m, 2H), 1.41 (s, 3H), 1.28 – 1.25 (m, 3H). ^{13}C NMR (151 MHz, DMSO-d_6) δ 161.87, 146.45, 144.22, 142.30, 130.51, 125.19, 123.28, 121.40, 120.90, 117.73, 115.38, 114.00 – 113.86, 77.74, 61.81, 31.29, 29.95, 24.52, 20.50, 13.32, 12.46, 12.26. ESI-MS *m/z*: 441.3 $[M+H]^+$; HRMS (ESI) *m/z* 441.2550 $[M+H]^+$ (calcd for 441.2548, $C_{26}H_{34}FN_2O_3$).

*N-(1-(4-fluorobenzyl)piperidin-4-yl)-6-hydroxy-2,5,7,8-tetramethylchromane-2-carboxamide (**5f**)*

Yield 35%, pale yellow oil. ^{1}H NMR (500 MHz, DMSO-d_6) δ 7.58 (s, 1H), 7.34 – 7.28 (m, 4H), 6.83 (d, J = 7.0 Hz, 1H), 3.58 – 3.55 (m, 1H), 3.29 – 3.26 (m, 2H), 2.57 (d, J = 7.9 Hz, 1H), 2.46 – 2.42 (m, 2H), 2.23 (dt, J = 14.2, 7.9 Hz, 2H), 2.13 (s, 3H), 2.12 (s, 3H), 2.01 (s, 3H), 1.74 – 1.72 (m, 2H), 1.47 – 1.45 (m, 2H), 1.41 (s, 3H), 1.26 – 1.25 (m, 3H). ^{13}C NMR (151 MHz, DMSO-d_6) δ 171.87, 146.45, 144.22, 142.30, 130.51, 125.19, 123.28, 121.40, 120.90, 117.73, 115.38, 113.86, 77.74, 61.81, 31.29, 29.95, 24.52, 20.50, 13.32, 12.46, 12.26. ESI-MS *m/z*: 441.3 $[M+H]^+$; HRMS (ESI) *m/z* 441.2545 $[M+H]^+$ (calcd for 441.2548, $C_{26}H_{34}FN_2O_3$).

*N-(1-(2,4-difluorobenzyl)piperidin-4-yl)-6-hydroxy-2,5,7,8-tetramethylchromane-2-carboxamide (**5g**)*

Yield 31%, white oil. ^{1}H NMR (500 MHz, DMSO-d_6) δ 7.58 (s, 1H), 7.37 – 7.35 (m, 2H), 7.23 (d, J = 7.3 Hz, 1H), 6.83 (d, J = 7.0 Hz, 1H), 3.60 – 3.57 (m, 1H),3.27 – 3.25 (m, 2H), 2.57 (d, J = 5.9 Hz, 1H), 2.46 – 2.36 (m, 2H), 2.24 – 2.22 (m, 2H), 2.13 (s, 3H), 2.12 (s, 3H), 2.01 (s, 3H), 1.95 – 1.93 (m,1H), 1.78 – 1.75 (m, 2H), 1.49 (dd, J = 13.1, 6.3 Hz, 2H), 1.41 (s, 3H), 1.25 – 1.21 (m, 3H). ^{13}C NMR (151 MHz, DMSO-d_6) δ 171.87, 146.45, 144.22, 142.30, 130.51, 125.19, 123.28, 121.40, 120.90, 117.73, 115.38, 113.86, 77.74, 61.81, 31.29, 29.95, 24.52, 20.50, 13.32, 12.46, 12.26. ESI-MS *m/z*: 459.3 $[M+H]^+$; HRMS (ESI) *m/z* 459.2457 $[M+H]^+$ (calcd for 459.2459, $C_{26}H_{33}F_2N_2O_3$).

*N-(1-(3,4-difluorobenzyl)piperidin-4-yl)-6-hydroxy-2,5,7,8-tetramethylchromane-2-carboxamide (**5h**)*

Yield 40%, white oil. ^{1}H NMR (500 MHz, DMSO-d_6) δ 7.58 (s, 1H), 7.36 (m, 2H), 7.23 (d, J = 7.3 Hz, 1H), 6.83 (d, J = 7.2 Hz, 1H), 3.58 – 3.56 (m, 1H), 3.29 – 3.27 (m, 2H), 2.57 (d, J = 5.9 Hz, 1H), 2.46 – 2.36 (m, 2H), 2.21 (dt, J = 11.9, 7.4 Hz, 2H), 2.13 (s, 3H), 2.12 (s, 3H), 2.01 (s, 3H), 1.96 –1.93(m, 1H), 1.78 – 1.75 (m, 2H), 1.49 (dd, J = 10.6, 7.3 Hz, 2H), 1.41 (s, 3H), 1.30 – 1.27 (m, 3H). ^{13}C NMR (151 MHz, DMSO-d_6) δ 171.87, 146.45, 144.22, 142.30, 130.51, 125.19, 123.28, 121.40, 120.90, 117.73, 115.38, 113.86, 77.74, 61.81, 31.29, 29.95, 24.52, 20.50, 13.32, 12.46, 12.26. ESI-MS *m/z*: 459.3 $[M+H]^+$; HRMS (ESI) *m/z* 459.2456 $[M+H]^+$ (calcd for 459.2459, $C_{26}H_{33}F_2N_2O_3$).

*N-(1-(2-chlorobenzyl)piperidin-4-yl)-6-hydroxy-2,5,7,8-tetramethylchromane-2-carboxamide (**5i**)*

Yield 33%, white oil. ^{1}H NMR (500 MHz, DMSO-d_6) δ 7.58 (s, 1H), 7.36 (dd, J = 14.5, 7.3 Hz, 1H), 7.15 – 7.12 (m, 3H), 6.82 (d, J = 7.3 Hz, 1H), 3.58 – 3.54 (m, 1H), 3.38 – 3.36 (m, 1H), 3.32 (d, J = 9.5 Hz, 1H), 2.64 – 2.61 (m, 1H), 2.46 – 2.44 (m, 2H), 2.30 – 2.27 (m, 2H), 2.13 (d, J = 4.4 Hz, 6H), 2.01 (s, 3H), 1.80 – 1.77 (m, 2H), 1.49 (dd, J = 10.6, 7.2 Hz, 2H), 1.39 (d, J = 12.1 Hz, 4H), 1.29 – 1.26 (m, 2H). ^{13}C NMR (151 MHz, DMSO-d_6) δ 172.88, 146.42, 141.85, 139.32, 133.42, 130.62, 128.70, 127.82, 127.28, 121.46, 77.79, 61.70, 29.95, 24.62, 20.62, 13.29, 12.46, 12.26. ESI-MS *m/z*: 457.2 $[M+H]^+$; HRMS (ESI) *m/z* 457.2255 $[M+H]^+$ (calcd for 457.2252, $C_{26}H_{34}ClN_2O_3$).

*N-(1-(3-chlorobenzyl)piperidin-4-yl)-6-hydroxy-2,5,7,8-tetramethylchromane-2-carboxamide(**5j**)*

Yield 36%, white oil. ^{1}H NMR (500 MHz, DMSO-d_6) δ 7.58 (s, 1H), 7.36 (d, J = 7.3 Hz, 1H), 7.28 – 7.26 (m, 3H), 6.82 (d, J = 7.3 Hz, 1H), 3.58 (d, J = 4.0 Hz, 1H), 3.38 – 3.36 (m, 1H), 3.32 (d, J = 9.5 Hz, 1H), 2.54 – 2.52 (m, 1H), 2.35 – 2.31 (m, 2H), 2.28 – 2.24 (m, 2H), 2.12 (d, J = 4.4 Hz, 6H), 2.01 (s, 3H), 1.79 – 1.76 (m, 2H), 1.49 – 1.45 (m, 2H), 1.39 (d, J = 12.1 Hz, 4H), 1.30 – 1.28 (m, 2H). ^{13}C NMR (151 MHz, DMSO-d_6) δ 172.88, 146.42, 141.85, 139.32, 133.42, 130.62, 128.70, 127.82, 127.28, 121.46, 77.79, 61.70, 29.95, 24.62, 20.62, 13.29, 12.46, 12.26. ESI-MS *m/z*: 457.2 $[M+H]^+$; HRMS (ESI) *m/z* 457.2254 $[M+H]^+$ (calcd for 457.2252, $C_{26}H_{34}ClN_2O_3$).

*N-(1-(4-bromobenzyl)piperidin-4-yl)-6-hydroxy-2,5,7,8-tetramethylchromane-2-carboxamide (**5k**)*

Yield 35%, white oil. ^{1}H NMR (500 MHz, DMSO-d_6) δ 7.58 (s, 1H), 7.36 (d, J = 7.3 Hz, 1H), 7.04 – 7.01 (m, 3H), 6.82 (d, J = 7.2 Hz, 1H), 3.59 – 3.58(m, 1H), 3.38 (d, J = 13.8 Hz, 1H), 3.31 (d, J = 13.4 Hz, 1H), 2.55 (dd, J = 12.4, 6.6 Hz, 1H), 2.47 – 2.45 (m, 2H), 2.17 – 2.15(m, 2H), 2.12 (s, 3H), 2.11 (s, 3H) 2.01 (s, 3H), 1.68 – 1.65 (m, 2H), 1.50 – 1.47 (m, 2H), 1.41 (s, 3H), 1.40 – 1.37 (m, 1H), 1.29 – 1.26 (m, 2H). ^{13}C NMR (151 MHz, DMSO-d_6) δ 172.93, 146.50, 144.27, 139.03, 129.17, 128.58, 127.29, 123.22, 121.34, 120.94, 117.86, 77.89, 62.45, 31.14, 29.99, 24.72, 20.42, 13.25, 12.42, 12.23. ESI-MS *m/z*: 501.2 $[M+H]^+$; HRMS (ESI) *m/z* 501.1751 $[M+H]^+$ (calcd for 501.1753, $C_{26}H_{34}BrN_2O_2$).

*6-hydroxy-2,5,7,8-tetramethyl-N-(1-(4-nitrobenzyl)piperidin-4-yl)chromane-2-carboxamide (**5l**)*

Yield 41%, pale brown oil. ^{1}H NMR (500 MHz, DMSO-d_6) δ 8.13 (s, 1H), 8.12 (s, 1H), 7.73 (d, J = 7.6 Hz, 1H), 7.63 (t, J = 7.8 Hz, 1H), 7.57 (s, 1H), 6.86 (d, J = 7.1 Hz, 1H), 3.64 – 3.59 (m, 1H), 3.48 – 3.45 (m, 2H), 2.55 (dd, J = 12.4, 6.6 Hz, 1H), 2.36 – 2.33 (m, 2H), 2.27 – 2.24 (m, 2H), 2.12 (d, J = 4.4 Hz, 6H), 2.01 (s, 3H), 1.78 – 1.75 (m, 2H), 1.50 – 1.47(m, 2H), 1.41 (s, 3H), 1.39 –1.36 (m, 1H), 1.30 – 1.25 (m, 2H). ^{13}C NMR (151 MHz, DMSO-d_6) δ 173.18, 148.28 , 146.48 , 144.30, 135.71, 130.24, 123.31, 123.19, 122.37, 121.40, 120.91, 118.53, 117.71, 77.83, 61.22 , 31.11, 30.20, 24.59, 20.78, 13.39, 12.45, 12.2. ESI-MS *m/z*: 468.3 $[M+H]^+$; HRMS (ESI) *m/z* 468.2496 $[M+H]^+$ (calcd for 468.2493, $C_{26}H_{34}N_3O_5$).

*N-(1-benzylpiperidin-4-yl)-6-hydroxy-2,5,7,8-tetramethylchromane-2-carboxamide (**5m**)*

^{1}H NMR (500 MHz, DMSO-d_6) δ 7.56 (s, 1H), 7.35 – 7.29 (m, 2H), 7.29 – 7.22 (m, 3H), 6.80 (d, J = 7.5 Hz, 1H), 3.63 – 3.54 (m, 1H), 3.30 (d, J = 11.5 Hz, 2H), 3.19 (d, J = 5.2 Hz, 1H), 2.56 (dd, J = 11.5, 5.6 Hz, 1H), 2.47 – 2.44 (m, 2H), 2.25 – 2.20 (m, 2H), 2.13 (s, 3H), 2.12 (s, 3H), 2.01 (s, 3H), 1.98 (s, 1H), 1.79 – 1.66 (m, 2H), 1.52 – 1.50 (m, 2H), 1.41 (s, 3H), 1.32 – 1.30 (m, 1H).^{13}C NMR (151 MHz, DMSO-d_6) δ 172.93, 146.50, 144.27, 139.03, 129.17, 128.58, 127.29, 123.22, 121.34, 120.94, 117.86, 77.89, 62.45, 31.14, 29.99, 24.72, 20.42, 13.25, 12.42, 12.23. ESI-MS *m/z*: 423.3 $[M+H]^+$; HRMS (ESI) *m/z* 423.2640 $[M+H]^+$ (calcd for 423.2642, $C_{26}H_{35}N_2O_3$).

*6-hydroxy-N-(2-(1-(4-methoxybenzyl)piperidin-4-yl)ethyl)-2,5,7,8-tetramethylchromane-2-carboxamide (**6a**)*

Yield 45%, white oil. ^{1}H NMR (500 MHz, DMSO-d_6) δ 7.49 (s, 1H), 7.15 (d, J = 8.5 Hz, 2H), 7.07 (t, J = 5.8 Hz, 1H), 6.85 (d, J = 8.6 Hz, 2H), 3.72 (s, 3H), 3.59 (s, 1H), 3.28 (s, 2H), 3.17 (s, 1H), 2.95 (dd, J = 12.2, 6.8 Hz, 1H), 2.62 (d, J = 11.0 Hz, 2H), 2.40 – 2.38 (m, 1H), 2.26 – 2.24 (m, 1H), 2.09 (s, 3H), 2.07 (s, 3H), 1.98 (s, 3H), 1.97 (m, 1H), 1.79 (s, 1H), 1.64 (m, 2H), 1.50 – 1.46 (m, 1H), 1.38 (s, 3H), 1.26 – 1.22 (m, 3H), 0.98 – 0.95 (m, 2H). ^{13}C NMR (151 MHz, DMSO-d_6) δ 173.58, 146.67, 144.22, 139.27, 129.32, 128.60, 127.13, 122.77, 120.23, 117.80, 77.82, 63.01, 55.43, 53.46, 49.15, 36.04, 32.49, 32.09, 29.83, 25.31, 20.73, 13.31, 12.39,12.33. ESI-MS *m/z*: 481.3 $[M+H]^+$; HRMS (ESI) *m/z* 481.3004 $[M+H]^+$ (calcd for 481.3006, $C_{29}H_{41}N_2O_4$).

6-hydroxy-2,5,7,8-tetramethyl-N-(2-(1-(2-methylbenzyl)piperidin-4-yl)ethyl)chro

*mane-2-carboxamide (**6b**)*

Yield 43%, white oil. ^{1}H NMR (500 MHz, DMSO-d_6) δ 7.53 (s, 1H), 7.19 – 7.17 (m, 1H), 7.11 – 7.02 (m, 4H), 3.34 (s, 2H), 3.21 (s, 1H), 2.95 (s, 1H), 2.65 (d, J = 10.9 Hz, 2H), 2.44 (s, 1H), 2.31 (s, 3H), 2.28 – 2.24 (m, 1H), 2.12 (d, J = 11.0 Hz, 6H), 2.02 (s, 3H), 1.82 (s, 1H), 1.68 – 1.64 (m, 3H), 1.50 – 1.48 (m, 1H), 1.41 (s, 3H), 1.39 (s, 1H), 1.22 – 1.20 (m, 2H), 0.97 – 0.95 (m, 2H), 0.77 – 0.76 (m, 1H). ^{13}C NMR (151 MHz, DMSO-d_6) δ 173.38, 146.51, 144.31, 137.38, 130.42, 129.88 , 127.21, 125.80, 122.85, 121.48, 120.50, 53.64, 36.10, 32.44, 32.17, 29.81, 25.39, 20.76, 19.27, 13.34, 12.46, 12.35. ESI-MS *m/z*: 465.3 $[M+H]^+$; HRMS (ESI) *m/z* 465.3114 $[M+H]^+$ (calcd for 465.3117, $C_{29}H_{41}N_2O_3$).

*6-hydroxy-2,5,7,8-tetramethyl-N-(2-(1-(4-methylbenzyl)piperidin-4-yl)ethyl)chromane-2-carboxamide (**6c**)*

Yield 39%, white oil. ^{1}H NMR (500 MHz, DMSO-d_6) δ 7.53 (s, 1H), 7.22 – 7.19 (m, 1H), 7.16 –7.12(m, 3H) 7.09 (t, J = 5.8 Hz, 1H), 3.34 (s, 2H), 3.21 (s, 1H), 2.95 (s, 1H), 2.65 (d, J = 10.9 Hz, 2H), 2.44 (s, 1H), 2.31 (s, 3H), 2.26 – 2.24(m, 1H), 2.12 (d, J = 11.4 Hz, 6H), 2.02 (s, 3H), 1.82 (s, 1H), 1.68 – 1.65 (m, 3H), 1.53 (s, 1H), 1.41 (s, 3H), 1.39 (s, 1H), 1.27 –1.25 (m, 2H), 1.01 – 0.97 (m, 2H), 0.77 – 0.76 (m, 1H). ^{13}C NMR (151 MHz, DMSO-d_6) δ 173.38, 146.51, 144.31, 137.38, 130.42, 129.88, 127.21, 125.80, 122.85, 121.48, 120.50, 53.64 , 36.10, 32.44, 32.01, 29.81, 25.39, 20.76, 19.27, 13.34, 12.46, 12.37. ESI-MS *m/z*: 465.3 $[M+H]^+$; HRMS (ESI) m/z 465.3114 $[M+H]^+$ (calcd for 465.3117, $C_{29}H_{41}N_2O_3$).

N-(2-(1-(2-fluorobenzyl)piperidin-4-yl)ethyl)-6-hydroxy-2,5,7,8-tetramethylchrom

*ane-2-carboxamide (**6d**)*

Yield 38%, white oil. ^{1}H NMR (500 MHz, DMSO-d_6) δ 7.51 (s, 1H), 7.38 (d, J = 7.4 Hz, 1H), 7.31 (d, J = 7.8 Hz, 1H), 7.23 –7.19 (m, 2H), 7.08 (t, J = 5.8 Hz, 1H), 3.45 (s, 2H), 3.22 (d, J = 6.7 Hz, 1H), 2.98– 2.95 (m, 1H), 2.68 (d, J = 11.1 Hz, 2H), 2.45 – 2.42 (m, 2H), 2.26 (dt, J = 10.8, 5.4 Hz, 1H), 2.12 (s, 3H), 2.09 (s, 3H), 2.01 (s, 3H), 1.73 (t, J = 11.5 Hz, 2H), 1.68 (d, J = 5.1 Hz, 1H), 1.40 (s, 3H), 1.25 – 1.20 (m, 4H), 1.01 – 0.97 (m, 2H), 0.76 – 0.73 (m, 1H). ^{13}C NMR (151 MHz, DMSO-d_6) δ 173.36, 162.19, 160.24, 146.31, 144.32, 131.88, 129.30, 125.67, 124.54, 122.88, 121.48, 120.53, 117.65, 115.48, 55.38, 53.37, 36.15, 32.37, 32.13, 29.87, 25.30, 20.74, 13.30, 12.43, 12.30. ESI-MS *m/z*: 469.3 $[M+H]^+$; HRMS (ESI) m/z 469.2864 $[M+H]^+$ (calcd for 469.2861, $C_{28}H_{38}FN_2O_3$).

*N-(2-(1-(3-fluorobenzyl)piperidin-4-yl)ethyl)-6-hydroxy-2,5,7,8-tetramethylchromane-2-carboxamide (**6e**)*

Yield 37%, white oil. ^{1}H NMR (500 MHz, DMSO-d_6) δ 7.51 (s, 1H), 7.36 – 7.34 (m, 1H), 7.31 (d, J = 7.8 Hz, 1H), 7.17 –7.14 (m, 2H), 7.08 (t, J = 5.8 Hz, 1H), 3.45 (s, 2H), 3.25 (d, J = 6.7 Hz, 1H), 2.93 – 2.90 (m, 1H), 2.69 (d, J = 11.5 Hz, 2H), 2.47 – 2.44 (m, 1H), 2.37 – 2.34 (m, 1H), 2.22 (dt, J = 11.2, 5.9 Hz, 1H), 2.12 (s, 3H), 2.09 (s, 3H), 2.01 (s, 3H), 1.70 – 1.68 (m, 2H), 1.68 (d, J = 5.1 Hz, 1H), 1.44(s, 3H), 1.27 – 1.21 (m, 4H), 0.99 – 0.95 (m, 2H), 0.73 – 0.71 (m, 1H). ^{13}C NMR (151 MHz, DMSO-d_6) δ 173.36, 162.19, 160.24, 146.31, 144.32, 131.88, 129.30, 125.67, 124.54, 122.88, 121.48, 120.53, 117.65, 115.48, 55.38, 53.37, 36.15, 32.37, 32.13, 29.87,

25.30, 20.74, 13.30, 12.43, 12.32. ESI-MS *m/z*: 469.3 $[M+H]^+$; HRMS (ESI) *m/z* 469.2860 $[M+H]^+$ (calcd for 469.2861, $C_{28}H_{38}FN_2O_3$).

*N-(2-(1-(4-fluorobenzyl)piperidin-4-yl)ethyl)-6-hydroxy-2,5,7,8-tetramethylchromane-2-carboxamide (**6f**)*

Yield 36%, white oil. ^{1}H NMR (500 MHz, DMSO-d_6) δ 7.56 (s, 1H), 7.35 (d, J = 7.8 Hz, 1H), 7.31 (d, J = 7.8 Hz, 1H), 7.20 – 7.15 (m, 2H), 7.08 (t, J = 5.8 Hz, 1H), 3.45 (s, 2H), 3.22 (d, J = 6.7 Hz, 1H), 3.02 – 2.97 (m, 1H), 2.68 (d, J = 11.2 Hz, 2H), 2.49 – 2.46 (m, 2H), 2.24 (dt, J = 10.8, 5.3 Hz, 1H), 2.12 (s, 3H), 2.09 (s, 3H), 2.01 (s, 3H), 1.73 (m, 2H), 1.67 (d, J = 5.1 Hz, 1H), 1.40 (s, 3H), 1.23 – 1.19 (m, 4H), 0.96 –0.94 (m, 2H), 0.78 – 0.74 (m, 1H). ^{13}C NMR (151 MHz, DMSO-d_6) δ 173.36, 162.19, 160.24, 146.31, 144.32, 131.88, 129.30, 125.67, 124.54, 122.88, 121.48, 120.53, 117.65, 115.48, 55.38, 53.37, 36.15, 32.37, 32.19, 29.87, 25.30, 20.74, 13.30, 12.43. ESI-MS *m/z*: 469.3 $[M+H]^+$; HRMS (ESI) *m/z* 469.2862 $[M+H]^+$ (calcd for 469.2861, $C_{28}H_{38}FN_2O_3$).

*N-(2-(1-(2,4-difluorobenzyl)piperidin-4-yl)ethyl)-6-hydroxy-2,5,7,8-tetramethylchromane-2-carboxamide(**6g**)*

Yield 33%, white oil. ^{1}H NMR (500 MHz, DMSO-d_6) δ 7.59 (s, 1H), 7.39 (d, J = 7.8 Hz, 1H), 7.21 – 7.18 (m, 2H), 7.08 (t, J = 5.8 Hz, 1H), 3.45 (s, 2H), 3.29 (d, J = 13.1 Hz, 1H), 2.93 – 2.90 (m, 1H), 2.62 (d, J = 11.1 Hz, 2H), 2.46 – 2.44 (m,2H), 2.21 (dt, J = 11.4, 5.9 Hz, 1H), 2.12 (s, 3H), 2.09 (s, 3H), 2.01 (s, 3H), 1.76 –1.73 (m, 2H), 1.68 (d, J = 5.7Hz, 1H), 1.40 (s, 3H), 1.27 – 1.20 (m, 4H), 0.99 – 0.95 (m, 2H), 0.77 – 0.75 (m, 1H). ^{13}C NMR (151 MHz, DMSO-d_6) δ 173.36, 162.19, 160.24,

146.31, 144.32, 131.88, 129.30, 125.67, 124.54, 122.88, 121.48, 120.53, 117.65, 115.48, 55.38, 53.37, 36.15, 32.37, 32.13, 29.87, 25.30, 20.74, 13.30, 12.43, 12.35. ESI-MS *m/z*: 487.3 $[M+H]^+$; HRMS (ESI) *m/z* 487.2730 $[M+H]^+$ (calcd for 487.2733, $C_{28}H_{37}F_2N_2O_3$).

*N-(2-(1-(3,4-difluorobenzyl)piperidin-4-yl)ethyl)-6-hydroxy-2,5,7,8-tetramethylchromane-2-carboxamide (**6h**)*

Yield 31%, white oil. ^{1}H NMR (500 MHz, DMSO-d_6) δ 7.51 (s, 1H), 7.55 (d, J = 7.4 Hz, 1H), 7.19 – 7.13 (m, 2H), 7.08 (t, J = 5.8 Hz,1H), 3.55 (s, 2H), 3.22 (d, J = 12.7 Hz, 1H), 3.08 – 3.05 (m, 1H), 2.68 (d, J = 11.7 Hz, 2H), 2.54 – 2.51 (m, 1H), 2.45 – 2.42 (m, 1H), 2.26 (dt, J = 11.8, 5.9 Hz, 1H), 2.12 (s, 3H), 2.09 (s, 3H), 2.01 (s, 3H), 1.73 – 1.70 (m, 2H), 1.58 – 1.55 (m, 1H), 1.42 (s, 3H), 1.25 – 1.17 (m, 4H), 1.02 – 0.98 (m, 2H), 0.79 – 0.75 (m, 1H). ^{13}C NMR (151 MHz, DMSO-d_6) δ 173.36, 162.19, 160.24, 146.31, 144.32, 131.88, 129.30, 125.67, 124.54, 122.88, 121.48, 120.53, 117.65, 115.48, 55.38, 53.37, 36.15, 32.37, 32.13, 29.87, 25.30, 20.74, 13.30, 12.43, 12.27. ESI-MS *m/z*: 487.3 $[M+H]^+$; HRMS (ESI) m/z 487.2731 $[M+H]^+$ (calcd for 487.2733, $C_{28}H_{37}F_2N_2O_3$).

*N-(2-(1-(2-chlorobenzyl)piperidin-4-yl)ethyl)-6-hydroxy-2,5,7,8-tetramethylchromane-2-carboxamide(**6i**)*

Yield 31%, white oil.^{1}H NMR (500 MHz, DMSO-d_6) δ 7.52 (s, 1H), 7.33 (m, 3H), 7.25 (d, J = 7.4 Hz, 1H), 7.09 – 7.05 (t, J = 5.6 Hz, 1H), 3.40 (s, 2H), 3.25 (m, 1H), 2.96 (m, 1H), 2.65 (d, J = 10.9 Hz, 2H), 2.41 – 2.39 (m, 1H), 2.27 – 2.25 (m, 1H), 2.12 (s, 3H), 2.09 (s, 3H), 2.01 (s, 3H), 1.68 (dd, J = 12.9, 7.5 Hz, 4H), 1.40 (s, 3H),

1.35-1.30 (m,2H), 1.23-1.16 (m, 2H), 0.98 – 0.95 (m, 2H), 0.81 – 0.79 (m, 1H). ^{13}C NMR (151 MHz, DMSO-d_6) δ 173.36 , 146.40, 144.26, 142.06, 133.34, 130.44, 128.78, 127.59, 127.30, 122.85, 121.49, 120.50, 117.67, 77.78, 62.04, 55.41, 53.55, 36.06, 32.24, 31.79, 29.86, 25.32, 13.32, 12.44, 12.31. ESI-MS *m/z*: 485.3 $[M+H]^+$; HRMS (ESI) *m/z* 485.2570 $[M+H]^+$ (calcd for 485.2571, $C_{28}H_{38}ClN_2O_3$).

*N-(2-(1-(3-chlorobenzyl)piperidin-4-yl)ethyl)-6-hydroxy-2,5,7,8-tetramethylchromane-2-carboxamide(**6j**)*

Yield 35%, white oil. ^{1}H NMR (500 MHz, DMSO-d_6) δ 7.62 (s, 1H), 7.35 –7.30 (m, 3H), 7.27 (d, J = 7.4 Hz, 1H), 7.09 (t, J = 5.8 Hz,, 1H), 3.40 (s, 2H), 3.20 – 3.19 (m, 1H), 2.94 – 2.92 (m, 1H), 2.67 (d, J = 10.9 Hz, 2H), 2.43– 2.40 (m, 1H), 2.27 – 2.25 (m, 1H), 2.12 (s, 3H), 2.09 (s, 3H), 2.01 (s, 3H), 1.70 (dd, J = 12.9, 7.5 Hz, 4H), 1.39 (s, 5H), 1.25 – 1.21 (m, 2H), 0.98 – 0.95(m, 2H), 0.82– 0.79 (m, 1H). ^{13}C NMR (151 MHz, DMSO-d_6) δ 173.36, 146.40, 144.26, 142.06, 133.34, 130.44, 128.78, 127.75, 127.30, 122.85, 121.49, 120.50, 117.67, 77.78, 62.04, 55.41, 53.55, 36.06, 32.24, 31.98, 29.86 , 25.32, 13.32, 12.44. 12.33, 12.29. ESI-MS *m/z*: 485.3 $[M+H]^+$; HRMS (ESI) *m/z* 485.2572 $[M+H]^+$ (calcd for 485.2571, $C_{28}H_{38}ClN_2O_3$).

*N-(2-(1-(4-bromobenzyl)piperidin-4-yl)ethyl)-6-hydroxy-2,5,7,8-tetramethylchromane-2-carboxamide (**6k**)*

Yield 40%, white oil.^{1}H NMR (500 MHz, DMSO-d_6) δ 7.64 – 7.62 (m, 1H), 7.35 – 7.32 (m,1H) 7.29 – 7.25 (m, 3H), 7.10 (t, J = 5.8 Hz, 1H), 3.39 (s, 2H), 3.23 – 3.20 (m, 1H), 3.01 – 2.96 (m, 1H), 2.64 (d, J = 11.1 Hz, 2H), 2.48 – 2.46 (m, 1H), 2.30 (m, 1H), 2.12 (s, 3H), 2.09 (s, 3H), 2.01 (s, 3H), 1.64 – 1.60 (m, 3H), 1.41 (s, 3H), 1.29 –

1.25 (m, 4H), 1.03– 0.99 (m, 2H), 0.78 – 0.75 (m, 1H). ^{13}C NMR (151 MHz, DMSO-d_6) δ 173.37, 146.48, 144.31, 142.41, 131.63, 130.80, 129.97, 128.10, 122.80, 122.00, 121.49, 120.50, 117.70, 77.73, 61.75, 36.05, 32.29, 32.04, 29.86, 25.36, 20.75, 13.32, 12.44, 12.38. ESI-MS *m/z*: 529.2 $[M+H]^+$; HRMS (ESI) m/z 529.2064 $[M+H]^+$ (calcd for 529.2066, $C_{28}H_{38}BrN_2O_3$).

*6-hydroxy-2,5,7,8-tetramethyl-N-(2-(1-(4-nitrobenzyl)piperidin-4-yl)ethyl)chromane-2-carboxamide (**6l**)*

Yield 44%, brown oil.^{1}H NMR (500 MHz, DMSO-d_6) δ 7.84 – 7.80 (m, 1H), 7.66 (m, 1H), 7.60 (d, J = 6.7 Hz, 1H), 7.54 (m, 2H), 7.10 (t, J = 5.8 Hz, 1H), 3.64 (s, 2H), 3.21 (m, 1H), 2.98 (m, 1H), 2.42 (d, J = 9.7Hz, 1H), 2.26 – 2.24 (m, 1H), 2.12 (s, 3H), 2.11 (s, 2H), 2.09 (s, 3H), 2.00 (s, 3H), 1.76 – 1.71 (m, 3H), 1.40 (s, 3H), 1.36 – 1.33(m, 2H), 1.28– 1.25 (m, 1H), 1.19-1.16 (m, 2H), 0.87 – 0.84 (m, 2H), 0.75 – 0.72 (m, 1H). ^{13}C NMR (151 MHz, DMSO-d_6) δ 173.38, 150.04, 146.44, 144.29, 133.72, 132.95, 131.43, 124.50, 122.83, 121.50, 120.54, 117.81, 53.48, 36.11, 32.15, 32.00, 29.81, 25.29, 20.74, 13.41, 12.43, 12.37. ESI-MS *m/z*: 496.3 $[M+H]^+$; HRMS (ESI) *m/z* 496.2804 $[M+H]^+$ (calcd for 496.2806, $C_{28}H_{38}N_3O_5$).

*N-(2-(1-benzylpiperidin-4-yl)ethyl)-6-hydroxy-2,5,7,8-tetramethylchromane-2-carboxamide (**6m**)*

Yield 44%, white oil. ^{1}H NMR (500 MHz, DMSO-d_6) δ 7.52 (s, 1H), 7.34 – 7.29 (m, 3H), 7.28 – 7.22 (m, 2H), 7.07 (t, J = 5.8 Hz, 1H), 3.19 (d, J = 5.0 Hz, 2H), 2.96 (dd, J = 12.8, 5.9 Hz, 1H), 2.67 (d, J = 10.7 Hz, 2H), 2.45 – 2.44 (m, 1H), 2.30 – 2.26 (m, 1H), 2.12 (s, 3H), 2.10 (s, 3H), 2.01 (s, 3H), 1.67 (s, 3H), 1.41 (s, 6H), 1.21 (dd, J

= 14.4, 7.1 Hz, 2H), 1.05 – 0.94 (m, 2H), 0.91 – 0.83 (m, 2H), 0.77 – 0.71 (m, 1H). ^{13}C NMR (151 MHz, DMSO-d_6) δ 173.58, 146.67, 144.22, 139.27, 129.32, 128.60, 127.13, 122.77, 120.23, 117.80, 77.82, 63.01, 53.46, 49.15, 36.04, 32.49, 32.09, 29.83, 25.31, 20.73, 13.31, 12.39, 12.33. ESI-MS *m/z*: 451.3 $[M+H]^+$; HRMS (ESI) *m/z* 451.2957 $[M+H]^+$ (calcd for 451.2955, $C_{28}H_{39}N_2O_3$).

5. Supporting Information:

The pharmacology experimental procedures and supplementary tables and figures for the kinetic study on the mechanism of AChE inhibition by **6d,** the docking study of AChE, results for the PAMPA were available in supporting information.

6. Abbriviation Used

AD, Alzheimer's disease; ChEs, Cholinesterases; ACh, acetylcholine; AChE, acetylcholinesterase; BuChE, butyrylcholinesterase; AChEIs, acetylcholinesterase inhibitors; PAS, peripheral anionic site; CAS, catalytic anionic site; Aβ, β-amyloid; MAO-B, monoamine oxidase B; CNS, central nervous system; MTDLs, multi-target-directed ligands; ROS, reactive oxygen species; ThT, Thioflavin T; TEM, transmission electron microscopy; DPPH, diphenyl-1-picrylhydrazyl; ABTS, (2, 2'-azino-bis(3-ethylbenzthiazoline-6-sulfonicacid); ORAC, oxygen radical absorbance capacity; MTT, methyl thiazolyl tetrazolium; BBB, blood-brain barrier; PAMPA-BBB, parallel artificial membrane permeation; *D*-gal, *D*-galactose; AST,

aspartate aminotransferase; ALT, alanine aminotransferase; HE, hematoxylin and eosin; MOE, Molecular Operating Environment.

7. Author Information

* Correspondence Author

* Ling-Yi Kong. Tel/ Fax: +86-25-8327-1405. E-mail address: cpu_lykong@126.com

*Xiao-Bing Wang. Tel/ Fax: +86-25-8327-1402. E-mail address: xbwang@cpu.edu.cn

Author contributions statement

P. C., X. B. W. and L. Y. K. design the research; P. C. performed the research and drafted the manuscript. S. Q. F., X. L. Y., H. L. Y., J. J. W. and Q. H. L. participated in the experiments. H. H. provided the Morris water maze equipment. X. B. W. and L. Y. K. revised the paper. All authors read and approved the final manuscript.

Notes

The authors declare no competing financial interest.

8. Acknowledgements

This work is sponsored by the National Natural Science Foundation of China (81573313), the Qing Lan Project of Jiangsu Province in China, the Innovative Research Team in University (IRT_15R63) and the Priority Academic Program Development of Jiangsu Higher Education Institutions (PAPD).

9. References

(1) Finder, V. H. (2010) Alzheimer's disease: a general introduction and pathomechanism. *J. Alzheimers. Dis. 22* (Suppl 3), 5−19.

(2) Savelieff, M. G., Lee, S., Liu, Y., and Lim, M. H. (2013) Untangling β-amyloid , tau, and metals in Alzheimer's disease. *ACS Chem. Biol. 8*, 856−865.

(3) Kepp, K. P. (2012) Bioinorganic chemistry of Alzheimer's disease. *Chem. Rev. 112*, 5193−5239.

(4) Anand, R., Gill, K. D., and Mahdi, A. A. (2014) Therapeutics of Alzheimer's disease: Past, present and future. *Neuropharmacology. 76* (Part A), 27−50.

(5) Cavalli, A., Bolognesi, M. L., Minarini, A., Rosini, M., Tumiatti, V., Recanatini, M. and Melchiorre C. (2008) Multi-target-directed ligands to combat neurodegenerative diseases. *J. Med. Chem. 51*, 347-72.

(6) Klafki, H.W., Staufenbiel, M., Kornhuber, J., and Wiltfang, J. (2006) Therapeutic approaches to Alzheimer's disease. *Brain. 129*, 2840−2855.

(7) Inestrosa, N. C., Alvarez, A., Pérez, C. A., Moreno, R. D., Vicente, M., Linker, C., Casanueva, O. I., Soto, C., and Garrido, J. (1996) Acetylcholinesterase accelerates assembly of amyloidbeta-peptides into Alzheimer's fibrils: possible role of the peripheral site of the enzyme. *Neuron. 16*, 881−891.

(8) Alvarez, A., Alarcón, R., Opazo, C., Campos, E. O., Muñoz, F. J., Calderón, F. H., Daja, F., Gentry. M. K., Doctor, B. P., De Mello, F. G., and Inestrosa, N. C. (1998) Stable complexes involving acetylcholinesterase and amyloid-β peptide change the biochemical properties of the enzyme and increase the neurotoxicity of

Alzheimer's fibrils. *J. Neurosci. 18*, 3213−3223.

(9) Hardy, J., and Selkoe, D J. (2002) The amyloid hypothesis of Alzheimer's disease: progress and problems on the road to therapeutics. *Science 297*, 353−356.

(10) Shidore, M., Machhi, J., Shingala, K., Murumkar, P., Sharma, M. K., Agrawal, N., Tripathi, A., Parikh, Z., Pillai, P., and Yadav, M. R. (2016) Benzylpiperidine-linked diarylthiazoles as potential anti-Alzheimer's agents: synthesis and biological evaluation. *J. Med. Chem. 59*, 5823−5846.

(11) Ismaili, L., Refouvelet, B., Benchekroun, M., Brogi, S., Brindisi, M., Gemma, S. Campiani, G., Filipic, S., Agbaba, D., Esteban, G., Unzeta, M., NikolicButini , K., and MarcoContelles, S. J. (2016) Multitarget compounds bearing tacrine- and donepezil-like structural and functional motifs for the potential treatment of Alzheimer's disease. *Prog. Neurobiol. 151*, 4−34.

(12) Zha, X., Lamba, D., Zhang, L., Lou, Y., Xu, C., Kang, D., Chen, L., Xu, Y., Zhang，L., De Simone, A., Samez, S., Pesaresi, S., Stojan, J., Lopez, M. G., Egea, J., Andrisano,V., and Bartolini, M. (2016) Novel tacrine−benzofuran hybrids as potent multitarget-directed ligands for the treatment of Alzheimer's disease: design, synthesis, biological evaluation, and X-ray crystallography. *J. Med.Chem. 59*, 114−131.

(13) Bonda, D. J., Wang, X. L., Perry, G., Nunomura, A., Tabaton, M., Zhu, X. W., and Smith, M. A. (2010) Oxidative stress in Alzheimer disease: a possibility for prevention. *Neuropharma. 59*, 290−294.

(14) Gu, F., Zhu, M., Shi, J., Hu, Y., and Zhao, Z. (2008) Enhanced oxidative stress is

an early event during development of Alzheimer-like pathologies in presenilin conditional knock-out mice. *Neurosci. Lett. 440*, 44–48.

(15) Moreira, P. I., Santos, M. S., Oliveira, C. R., Shenk, J. C., Nunomura, A., Smith, M. A., Zhu, X., and Perry, G. (2008) Alzheimer disease and the role of free radicals in the pathogenesis of the disease. *CNS Neurol. Disord.: Drug Targets. 7*, 3–10.

(16) Huang, X., Moir, R. D., Tanzi, R. E., Bush, A. I., and Rogers, J. T. (2004) Redox-active metals, oxidative stress, and Alzheimer's disease pathology. *Ann. N.Y. Acad. Sci. 1012*, 153−156.

(17) Ismaili, L., Refouvelet, B., Benchekroun, M., Brogi, S., Brindisi, M., Gemma, S., Campiani, G., Filipic, S., Agbaba, D., Esteban, G., Unzeta, M., Nikolic, K., Butini, S., and Marcocontelles, J. (2016) Multitarget compounds bearing tacrine- and donepezil-like structural and functional motifs for the potential treatment of Alzheimer's disease. *Prog. Neurobiol. 151*, 4−34.

(18) Cordes, T., Vogelsang, J., and Tinnefeld, P. (2009) On the Mechanism of Trolox as Antiblinking and Antibleaching Reagent. *J. Am. Chem. Soc. 131*, 5018-5019.

(19) Wu, T. W., Hashimoto, N., Wu, J., Carey, D., Li, R. K., Mickle, D. A., and Weisel, R. D. (1990) The Cytoprotective Effect of Trolox Demonstrated with Three Types of Human Cells. *Biochem. Cell Biol. 68*, 1189−1194.

(20) Quintanilla, R. A., Munoz, F. J., Metcalfe, M. J., Hitschfeld, M., Olivares, G., Godoy, J. A., and Inestrosa, N. C. (2005) Trolox and 17beta-estradiol protect against amyloid beta-peptide neurotoxicity by a mechanism that involves

modulation of the Wnt signaling pathway. *J. Biol. Chem. 280*, 11615−11625.

(21) Sung, S., Yao, Y., Uryu, K., Yang, H., Lee, V. M., Trojanowski, J. Q. and Pratic D. (2004) Early vitamin E supplementation in young but not aged mice reduces abeta levels and amyloid deposition in a transgenic model of Alzheimer's disease. *FASEB. J. 18*, 323-325.

(22) Skrzydlewska, E., and Farbiszewski, R. (1997) Trolox-derivative antioxidant protects against methanol-induced damage. *Fundam Clin Pharmacol 11*, 460−465.

(23) Cavalli, A., Bolognesi, M. L., Capsoni, S., Andrisano, V., Bartolini, M., Margotti, E., Cattaneo, A., Recanatini, M., and Melchiorre, C. (2007) A small molecule targeting the multifactorial nature of Alzheimer'sdisease. *Angew. Chem., Int. Ed. 46*, 3689−3692.

(24)Weinreb, O., Amit, T., Bar-Am, O., and Youdim, M. B. (2012) Ladostigil: Anovel multimodal neuroprotective drug with cholinesterase and brainselective monoamine oxidase inhibitory activities for Alzheimer'sdisease treatment. *Curr Drug Targets. 13*, 483−494.

(25) Viayna, E., Gómez, T., Galdeano, C., Ramírez, L., Ratia, M., Badia, A., Clos, M. V., Verdaguer, E., Junyent, F., Camins, A., Pallàs, M., Bartolini, M., Mancini, F., Andrisano, V., Arce, M. P., Rodríguez-Franco, M. I., Bidon-Chanal, A., Luque, F. J., Camps, P., and Muñoz-Torrero D. (2010) Novel huprine derivatives with inhibitory activity toward β-amyloid aggregation and formation as disease-modifying anti-alzheimer drug candidates. *Chemmedchem. 5*,

1855-1870.

(26) Xie, S. S., Lan, J. S., Wang, X. B., Jiang, N., Dong, G., Li, Z. R., Wang, K. D., Guo, P. P., and Kong, L. Y. (2015). Multifunctional tacrine-trolox hybrids for the treatment of alzheimer's disease with cholinergic, antioxidant, neuroprotective and hepatoprotective properties. *Eur. J. Med. Chem. 93*, 42−50.

(27) Wang, J., Wang, Z. M., Li, X. M., Li, F., Wu, J. J., Kong, L. Y., and Wang, X. B. (2016). Synthesis and evaluation of multi-target-directed ligands for the treatment of alzheimer's disease based on the fusion of donepezil and melatonin. *Bioorg Med Chem, 24*, 4324−4338.

(28) Bolognesi, M. L., Cavalli, A., Valgimigli, L., Bartolini, M., Rosini, M., Andrisano, V., Recanatini, M., and Melchiorre. C. (2007) Multi-target-directed drug design strategy: from a dual binding site acetylcholinesterase inhibitor to a trifunctional compound against Alzheimer's disease. *J. Med. Chem. 50*, 6446−6649.

(29) Sugimoto H, Tsuchiya Y, Higurashi K, Karibe, N., Iimura, Y, Sasaki, A., Yamanashi, Y., Ogura, H., and Kosasa, T. (1996) 1,4-Substituted piperidines as acetylcholinesterase inhibitors and their use for the treatment of Alzheimer's disease: EP, EP0296560.

(30) Galiano, S., Ceras, J., Cirauqui, N., Galiano, S., Ceras, J., Cirauqui, N., Pérez, S., Juanenea, L., Rivera, G., Aldana, I., and Monge, A. (2007) Novel series of substituted biphenylmethyl urea derivatives as MCH-R1 antagonists for the treatment of obesity. *Bioorgan. Med. Chem. 15*, 3896−3911.

(31) Chan, L. C., & Cox, B. G. (2007). Kinetics of amide formation through carbodiimide/N-hydroxybenzotriazole (HOBt) couplings. *J. Org. Chem. 72*, 8863-8869.

(32) Ali, R., Sheikha, I. A., Jabirb, N. R., and Kamal, M. A. (2012). Comparative Review of Decade's Research on Cholinesterase Inhibition. *Am. J. Neuroprotec. Neuroregen. 4*, 136-144.

(33) Ellman, G. L., Courtney, K. D., Andres, V., and Featherstone, R.M. (1961) A new and rapid colorimetric determination of acetylcholinesterase activity. *Biochem. Pharmacol. 7*, 88−95.

(34) Lane, R. M., Potkin, S. G., and Enz, A. (2006). Targeting acetylcholinesterase and butyrylcholinesterase in dementia. *Int. J. Neuropsychopharmacol, 9*, 101−124.

(35) Ramsay, R. R., Sablin, S. O., and Singer, T. P. (1995). Redox properties of the flavin cofactor of monoamine oxidases A and B and their relationship to the kinetic mechanism. *Prog. Brain. Res. 106*, 33−39.

(36) Bortolato, M., Chen, K., and Shih, J. C. (2008). Monoamine oxidase inactivation: from pathophysiology to therapeutics. *Adv. Drug Deliv. Rev. 60*, 1527–1533.

(37) Farina, R., Pisani, L., Catto, M., Nicolotti, O., Gadaleta, D., Denora, N., Sotootero, R., Mendezalvarez, E., Passos, C. D. S., Muncipinto, G., Altomare, C., Nurisso, A., Carrupt, P., and Carotti, A. (2015) Structure-based design and optimization of multitarget-directed 2H-chromen-2-one derivatives as potent inhibitors of monoamine oxidase B and cholinesterases. *J. Med. Chem. 58*, 5561−5578.

(38) Scherer, R., and Godoy, H. T. (2009). Antioxidant activity index (AAI) by the 2,2-diphenyl-1-picrylhydrazyl method. *Food Chem. 112*, 654-658.

(39) Miller, N. J., and Riceevans, C. (1997) Factors influencing the antioxidant activity determined by the ABTS•+ radical cation assay. *Free Radical Res. 26*, 195−199.

(40) Dávalos, A., Carmen Gómezcordovés, A., and Bartolomé, B. (2004). Extending applicability of the oxygen radical absorbance capacity (orac−fluorescein) assay. *J. Agric. Food. Chem. 52*, 48−54.

(41) Wang, Z. M., Cai, P., Liu, Q. H., Xu, D. Q., Yang, X. L., Wu, J. J., Kong, L. Y., and Wang, X. B. (2017) Rational modification of donepezil as multifunctional acetylcholinesterase inhibitors for the treatment of Alzheimer's disease. *Eur. J. Med. Chem. 123*, 282−297.

(42) Lu, C., Guo, Y., Yan, J., Luo, Z., Luo, H. B., Yan, M., Huang, L., and Li, X. (2013) Design, Synthesis, and Evaluation of Multitarget-Directed Resveratrol Derivatives for the Treatment of Alzheimer's Disease. *J. Med. Chem. 56*, 5843−5459.

(43) Nepovimova, E., Korabecny, J., Dolezal, R., Babkova, K., Ondrejicek. A., Jun, D., Sepsova, V., Horova, A., Hrabinova, M., Soukup, O., Bukum, N., Jost, P., Muckova, L., Kassa, J., Malinak, D., Andrs, M., and Kuca, K. (2015) Tacrine – trolox hybrids: a novel class of centrally active, non-hepatotoxic multi-target-directed ligands exerting anticholinesterase and antioxidant activities with low in vivo toxicity. *J. Med. Chem. 58*, 8985−9003.

(44) Wang, Z., Wang, Y., Wang, B., Li, W., Huang, L., & Li, X. (2015). Design, synthesis and evaluation of orally available clioquinol-moracin m hybrids as multi-target-directed ligands for cognitive improvement in a rat model of neurodegeneration in alzheimer's disease. *J. Med. Chem. 58*, 8616-8637.

(45) Pisani, L., Farina, R., Catto, M., Iacobazzi, R. M., Nicolotti, O., Cellamare, S., Mangiatordi, G. F., Denora, N., Soto-Otero, R., Siragusa, L., Altomare, C. D., and Carotti A. (2016) Exploring Basic Tail Modifications of Coumarin-based Dual Acetylcholinesterase-Monoamine Oxidase B Inhibitors: Identification of Water-soluble, Brain-permeant Neuroprotective Multitarget Agents. *J. Med. Chem. 58*, 6791−6806.

(46) Block, M. L., Zecca, L., and Hong, J. S. (2007) Microglia-mediated neurotoxicity: uncovering the molecular mechanisms. *Nat. Rev Neurosci. 8*, 57−69.

(47) Egea, J., Buendia, I., Parada, E., Navarro, E., Leon, R., and Lopez, M. G. (2015) Anti-inflammatory role of microglial alpha7 nAChRs and its role in neuroprotection. *Biochem. Pharmacol. 97*, 463−472.

(48) Godoy, J. A., Rios, J. A., Zolezzi, J. M., Braidy, N., and Inestrosa, N. C. (2014) Signaling pathway cross talk in Alzheimer's disease. *Cell Commun. Signal. 12*, 23−23.

(48) Sil, S., Ghosh, T., Ghosh,R., Ghosh, R., and Gupta, P. (2017) Nitric oxide synthase inhibitor, aminoguanidine reduces intracerebroventricular colchicine induced neurodegeneration, memory impairments and changes of systemic immune responses in rats. *J. Neuroimmunol. 303*, 51−61.

(49) Di, L., Kerns, E. H., Fan,K., Mcconnell, O., and Carter, G. T. (2003) High throughput artificial membrane permeability assay for blood–brain barrier. *Eur. J. Med. Chem. 38*, 223−232.

(50) Blokland, A. (2005). Scopolamine-induced deficits in cognitive performance: a review of animal studies. *Scopolamine Rev*.1-76

(51) Ukai, M., Kobayashi, T., Shinkai, N., Shan-Wu, X., and Kameyama, T. (1995) Dynorphin A-(1-13) potently improves scopolamine-induced impairment of passive avoidance response in mice, *Eur. J. Pharmacol. 274*, 89-93.

(52) Morris, R. (1984) Developments of a water-maze procedure for the studying spatial learning in the rat. *J. Neurosci. Methods. 11*, 47−60.

(53) Miao, H., Lin, Z., Wei, M. J., Yao, W. F., Zhao, H. S., and Chen, F. J. (2009) Neuroprotective effects of (-)-epigallocatechin-3-gallate on aging mice induced by D-galactose. *Biol Pharm Bull. 32*, 55−60.

(54) Savory, J., Herman, M. M., and Ghribi. O. (2006) Mechanisms of aluminum-induced neurodegeneration in animals: Implications for Alzheimer's disease. *J. Alzheimers Dis. 10*, 135−144.

(55) Xu, P., Wang, K., Lu, C., Dong, L., Gao, L., Yan, M. Aibai, S. Yang, Y., and Liu, X. (2017) The Protective Effect of Lavender Essential Oil and Its Main Component Linalool against the Cognitive Deficits Induced by D-Galactose and Aluminum Trichloride in Mice. *Evid Based Complement Alternat. Med. 2017*, 7426538.

(56) Yang,W. N., Han, H., Hu, X. D. Feng, G. F., and Qian, Y. H. (2013) The effects of

perindopril on cognitive impairment induced by d-galactose and aluminum trichloride via inhibition of acetylcholinesterase activity and oxidative stress. *Pharmacol Biochem Behav. 114-115*, 31−36.

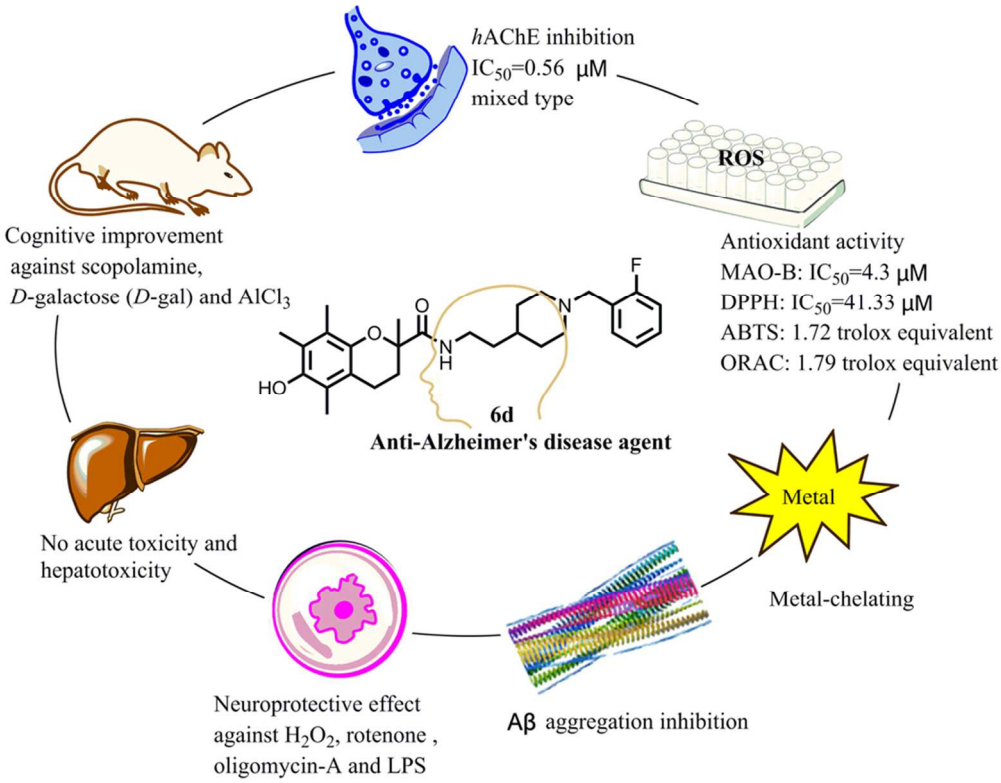

For Table of Contents Use Only

88x69mm (300 x 300 DPI)

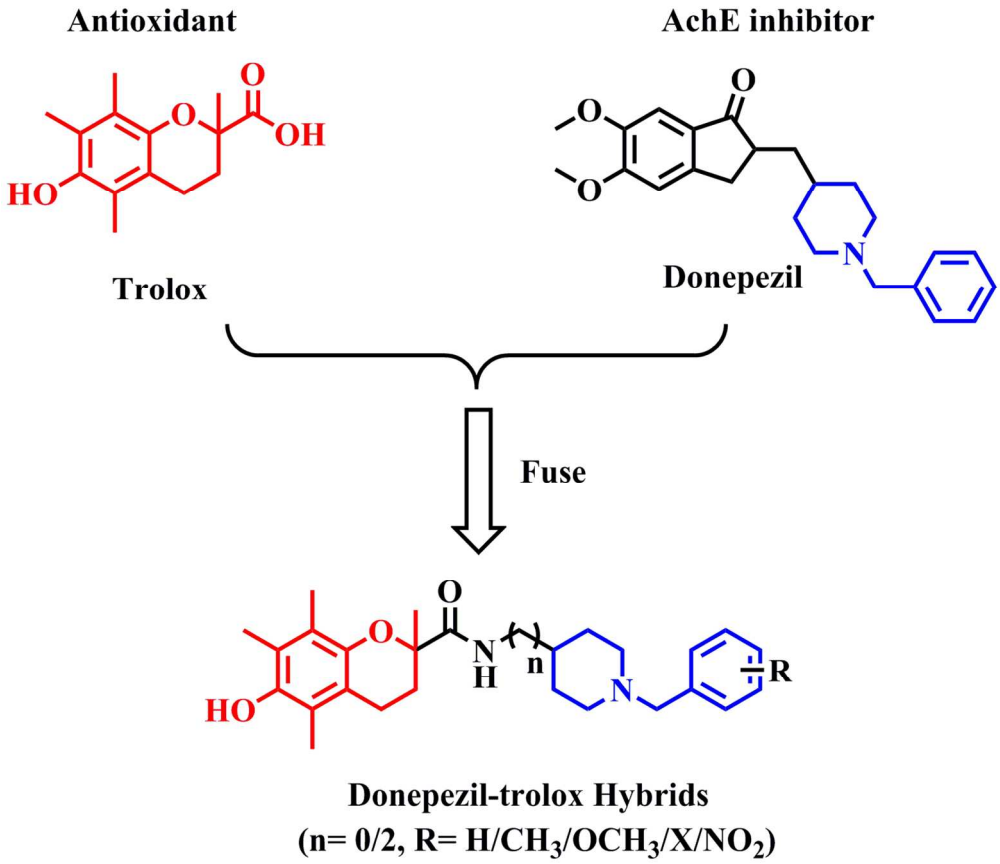

Figure 1. Design strategy of the multifunctional donepezil-trolox hybrids.

127x111mm (300 x 300 DPI)

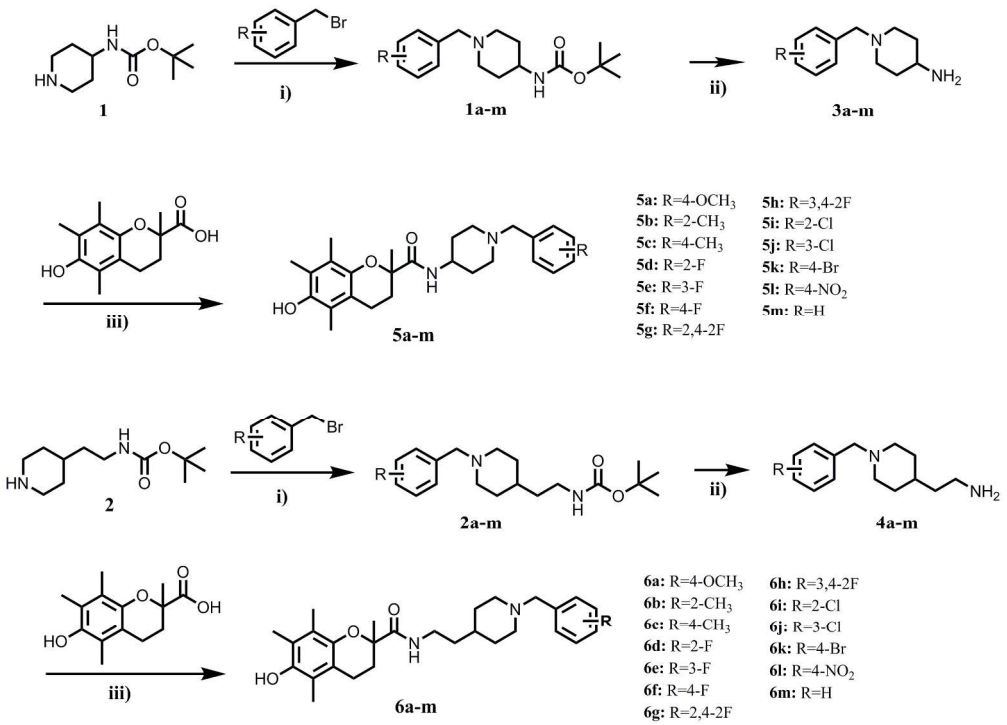

Scheme 1. Synthesis of the target compounds. Reagents and conditions: i) EtOH, TEA, r.t., 6h; ii) TFA, DCM, r,t., 4h; iii) HOBt/EDCI, DCM, r.t., 12h.

217x157mm (300 x 300 DPI)

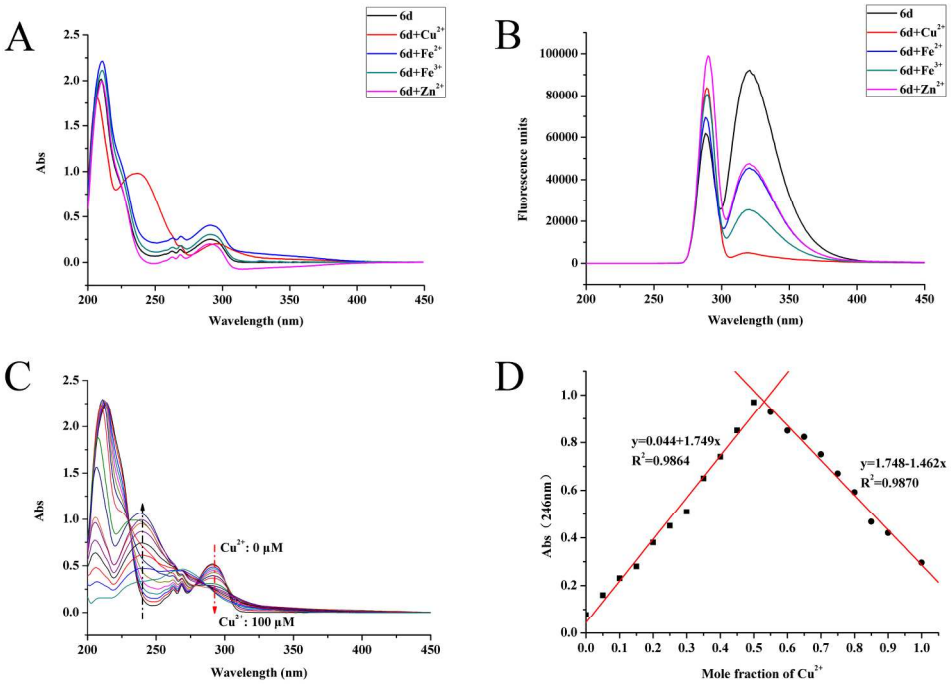

Figure 2. (A) UV absosobance spectrum of compound 6d (100 μM) alone or in the presence of CuSO4 (100 μM), ZnCl2 (100 μM), FeSO4 (100 μM), or FeCl3(100 μM) in buffer (20 mM HEPES, 150 mM NaCl, pH 7.4); (B) Fluorescence intensity of compound 6d (100 μM) alone and in the presence of CuSO4 (100 μM), ZnCl2 (100 μM), FeSO4 (100 μM), or FeCl3 (100 μM) in buffer (20 mM HEPES, 150 mM NaCl, pH 7.4). (C) UV−vis titration of compound 6d with Cu2+ in buffer (20 mM HEPES, 150 mM NaCl, pH 7.4) at room temperature. (D) Determination of the stoichiometry of complex Cu2+-6d by Job's method.

201x145mm (300 x 300 DPI)

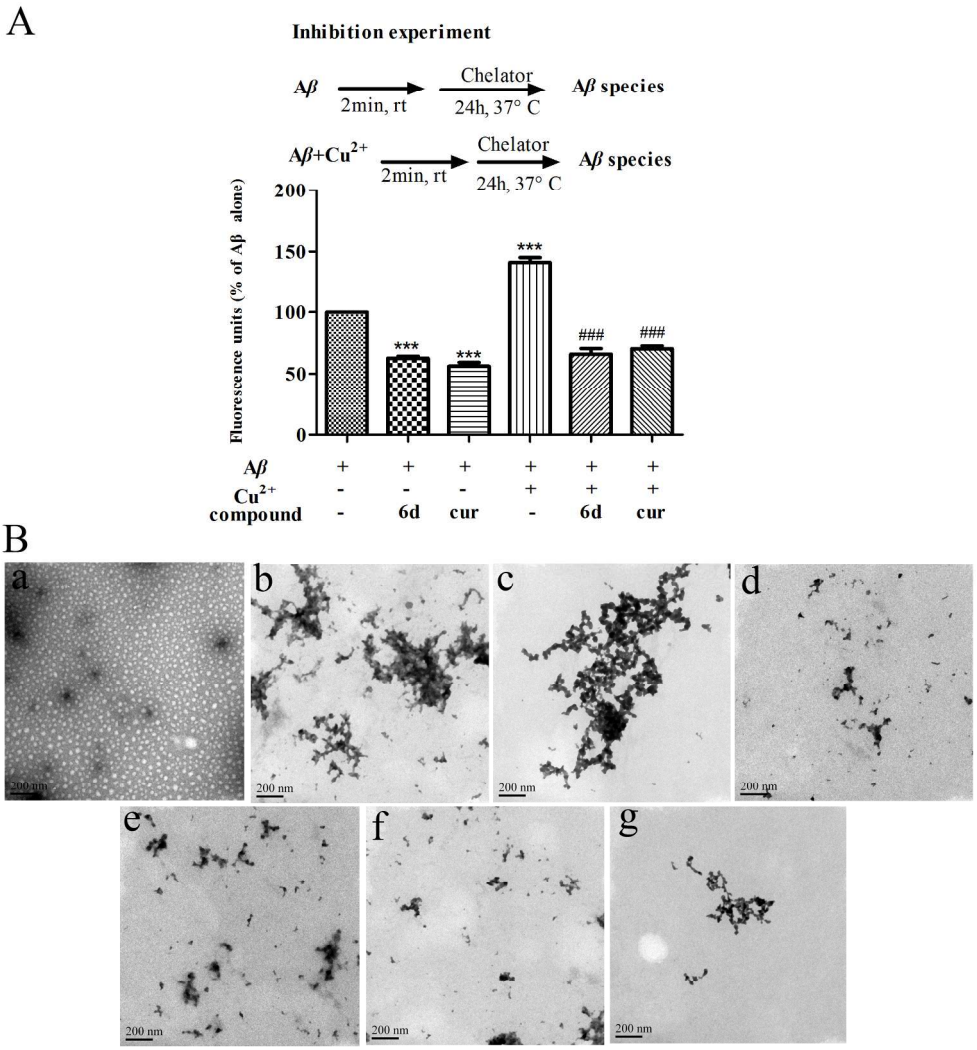

Figure 3. (A) Results of the ThT binding assay. Statistical significance was analyzed by ANOVA: (***p) < 0.001 versus Aβ1−42 alone, (###p) < 0.001versus Aβ1−42 + Cu2+, data are expressed as the mean ± SD at least three independent experiments. (B) TEM images analysis of the inhibition of self-induced and Cu2+-induced Aβ1-42 aggregates: (a) fresh Aβ1-42; (b)Aβ1-42 alone (c) Aβ1-42 + Cu2+; (d) Aβ1-42 +curcumin, (e) Aβ1-42 + Cu2+ + curcumin; (f) Aβ1-42 + 6d; (g) Aβ1-42 + Cu2+ + 6d.

207x225mm (300 x 300 DPI)

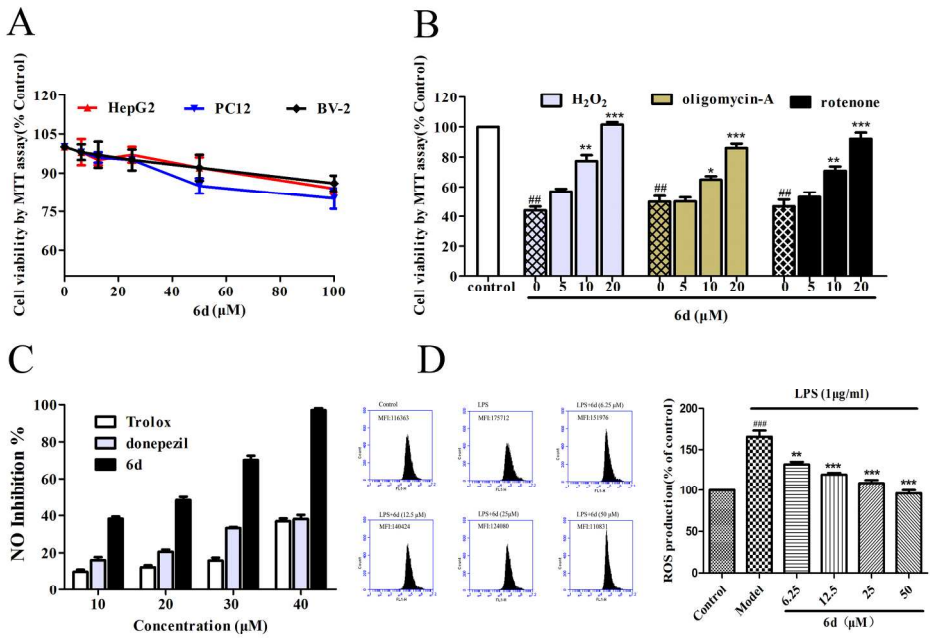

Figure 4. (A) Effects of compound 6d on cell viability in HepG-2, PC12 and BV-2 cells. Values are reported as the mean ± SD of three independent experiments. (B) Neuroprotective effect on PC12 cells of compound 6d after 24 h incubation at different concentrations (5, 10 and 20 μM) with H2O2 (100 μM), oligomycin-A (20 μM), and rotenone (200 μM). Data are expressed as percentage of viable cells (referred to control) and shown as mean ± SD (n = 3). Untreated cells were used as control. (C) The effect of compound 6d on LPS-stimulated production of inflammatory mediators NO in BV-2 cells. Griess assay was used to detect the suppression of NO production following LPS-induced inflammatory events in BV2 microglia cells using resveratrol, trolox and donepezil as a positive control. Results are expressed as percent of cells with solely treatment of LPS. (D) Effect of 6d against LPS-induced intracellular ROS accumulation was measured by DCFH-DA staining and analyzed by flow cytometry. Analysis of ROS production is presented as the meanfluorescence intensity (MFI). Data are presented by mean ± SD. (###p) ≤ 0.001 compared with the control group. (*p) ≤ 0.05 and (**p) ≤ 0.01 compared with 1 μg/ml LPS-treated group.

209x144mm (300 x 300 DPI)

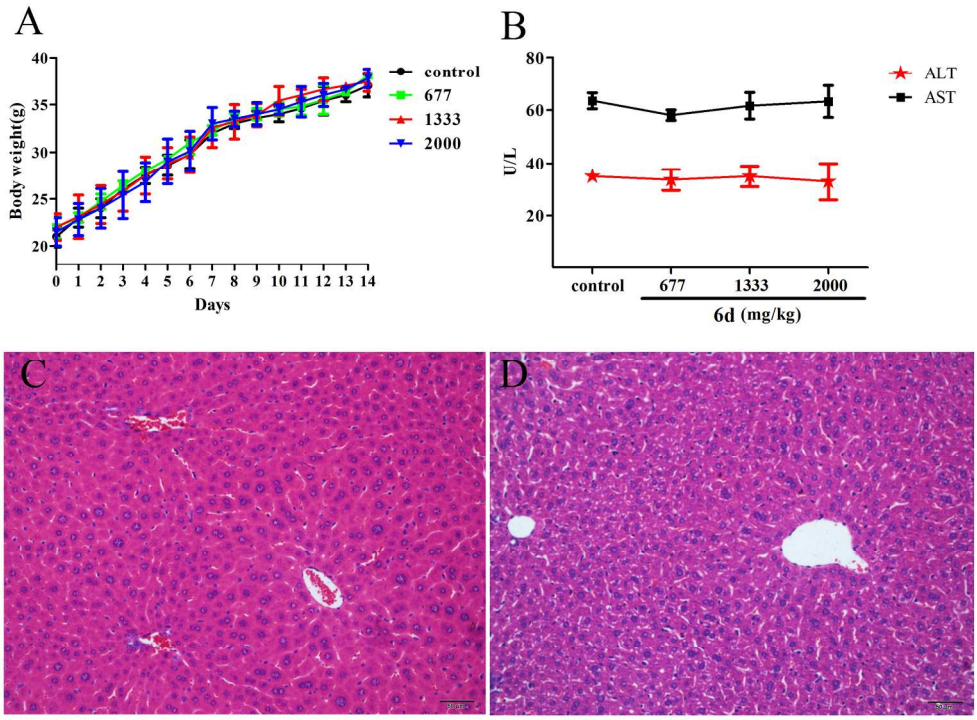

Figure 5. (A) The mean daily body weight profile of each group mice during the 14 day drug administration period. (B) The AST and ALT activity on the 14th day after completing tested the acute toxicity study with administration of three different dosage of the compound 6d. Results are expressed as mean ± SD (n=5). (C) and (D) Histomorphological appearance of livers of male mice after treatment with the solvent only (control) and the high dosage 2000mg/kg. HE, original magnification: × 200.

208x159mm (300 x 300 DPI)

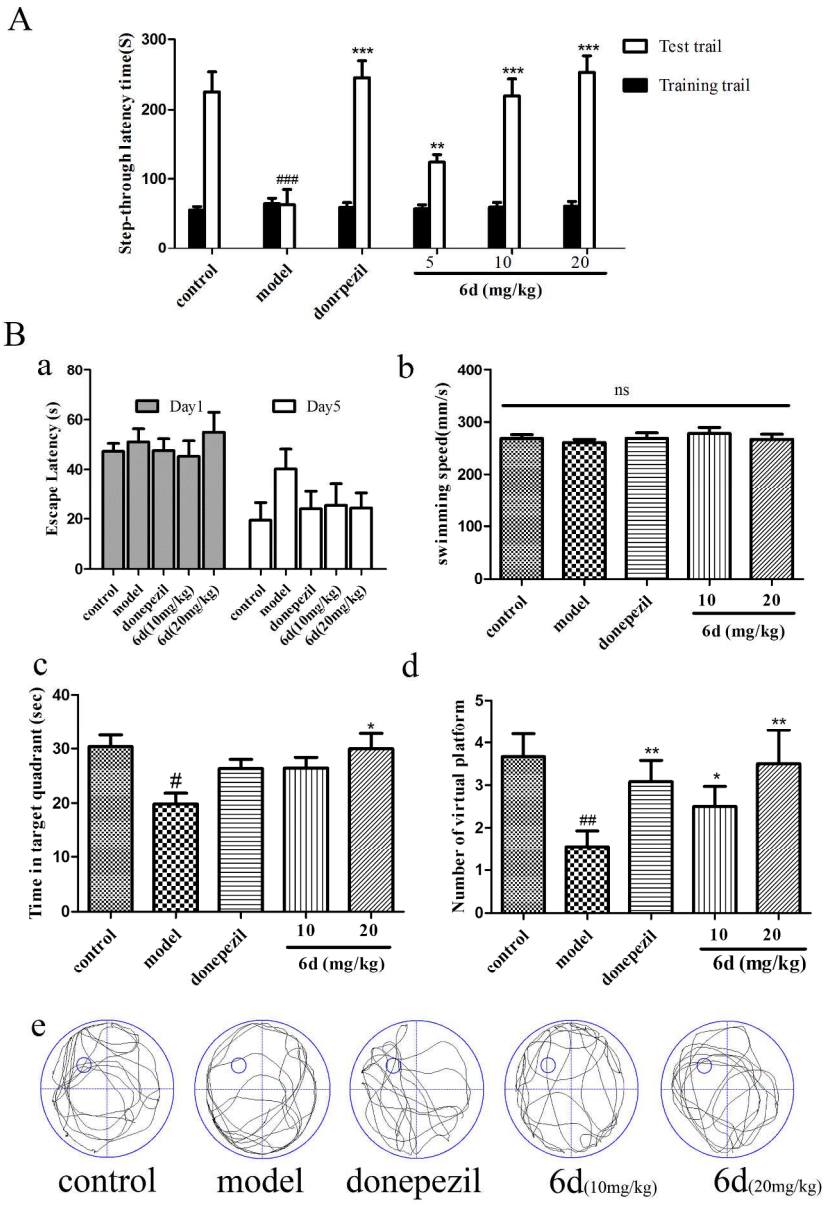

Figure 6. Scopolamine-induced memory deficit mice model study. (A) Effects of 6d on scopolamine-induced memory deficit in the step-through passive avoidance test. Compound 6d (both at 5, 10 and 20 mg/kg p.o.) and donepezil (5 mg/kg, p.o.) were orally given 30 min before treatment of scopolamine. After 60min, the mice were treated with scopolamine (3 mg/kg, i.p.) and tested in the step-through passive avoidance. Values are expressed as the mean ± SD (n =10). (###p) ≤ 0.001 compared with the control group. (*p) ≤ 0.05 and (**p) ≤ 0.01 compared with scopolamine - treated group. (B) Compound 6d attenuates scopolamine-induced spatial learning and memory deficits in the training session of Morris water maze task. Data are presented as the mean ± SD (n = 11-12); Statistical significance was analyzed by two-way ANOVA: (ns)p > 0.05, (##p) < 0.01 compared with control group, (*p)<0.05, (**p) < 0.01 compared with sham group. (a)The escape latency time of each group was counted on day 1 and day 5 during the period of training trial. (b) The average swimming speed for the rats. (c) The time spent in the virtual platform quadrant. (d) Number of virtual platform (the original platform location) crossings. (e) The representative tracks of the mice in Morris water maze during the spatial probe trial period. The location of the platform

and the effective region (2-fold diameter of the platform) were represented as a blue circles, respectively.

203x290mm (300 x 300 DPI)

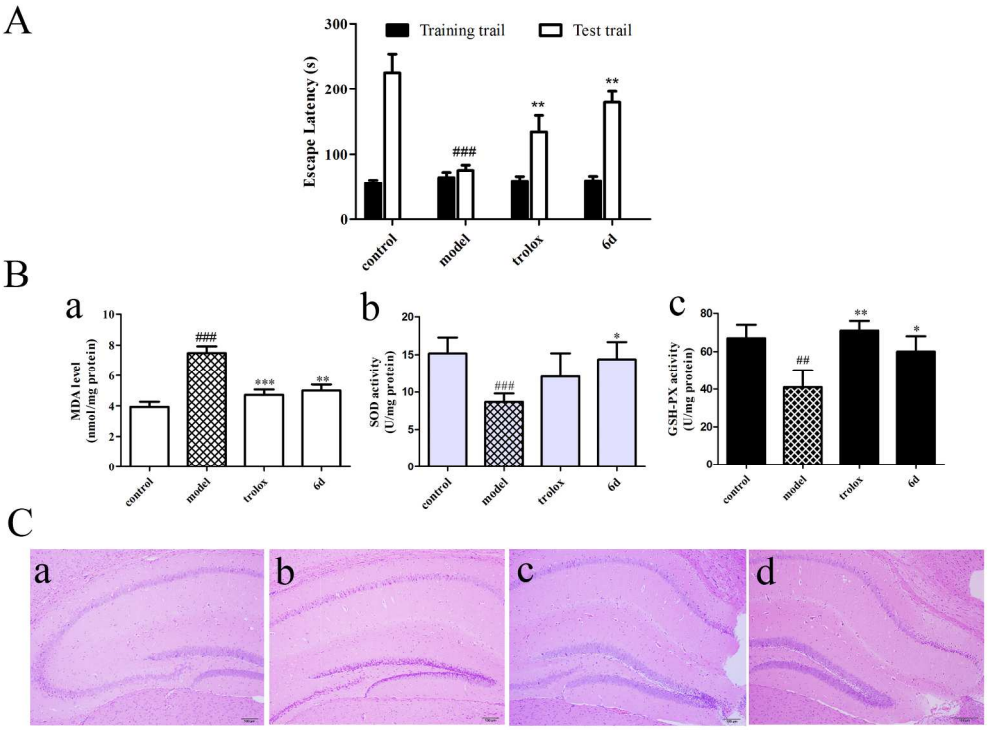

Figure 7. D-gal and AlCl3-induced memory deficit mice model study. (A) Effects of compound 6d on D-gal and AlCl3-induced memory deficit in the step-through passive avoidance test. Compound 6d (20 mg/kg p.o.) and donepezil (5 mg/kg, p.o.) were orally given 30 min before treatment of scopolamine. After 60min, the mice were treated with scopolamine (3 mg/kg, i.p.) and tested in the step-through passive avoidance. Values are expressed as the mean ± SD (n =10). (###p) ≤ 0.001 compared with the control group. (*p) ≤ 0.05 and (**p) ≤ 0.01 compared with scopolamine - treated group.(B) The biochemical analysis as follows: the MDA (a), SOD(b), GSH-PX (c) in each group with research effects of 6d in brain of D-gal and AlCl3 treated mice. Values are expressed as the mean ± SD (n =10). (###p)≤ 0.001, (##)p≤ 0.01 compared with the control group. (*p) ≤ 0.05 and (**p) ≤ 0.01 compared with D-gal and AlCl3 - treated group. (C) Histomorphological appearance of hippocampal neurons of male mice after treatment with the solvent only (control) (a) and model group(b), and administration of trolox (c) and 6d (d). H&E, originalmagnification:× 200.

209x157mm (300 x 300 DPI)